LEVEL

FINAL TECHNICAL REPORT

⑫

on

EFFECTS OF HOT FORGING VARIABLES UPON MICROSTRUCTURE
AND PROPERTIES OF METALS AND ALLOYS

(Grant No. AFOSR-76-2971)

to

AIR FORCE OFFICE OF SCIENTIFIC RESEARCH
Bolling Air Force Base
Washington, D. C.

February 23, 1979

DDC
MAR 14 1979

by

T. Altan, A. H. Clauer, G. D. Lahoti,
A. R. Rosenfield, and T. L. Subramanian

BATTELLE
Columbus Laboratories
505 King Avenue
Columbus, Ohio 43201

79 03 12 061

REPORT DOCUMENTATION PAGE		READ INSTRUCTIONS BEFORE COMPLETING FORM
1. REPORT NUMBER **AFOSR-TR- 79-0239**	2. GOVT ACCESSION NO.	3. RECIPIENT'S CATALOG NUMBER
4. TITLE (and Subtitle) Effects of Hot Forging Variables Upon Microstructure and Properties of Metals and Alloys		5. TYPE OF REPORT & PERIOD COVERED Final Jan 1, 1976 - Dec 31, 1978
		6. PERFORMING ORG. REPORT NUMBER
7. AUTHOR(s) T. Altan, A. H. Clauer, G. D. Lahoti, A. R. Rosenfield, T. L. Subramanian		8. CONTRACT OR GRANT NUMBER(s) AFOSR-76-2971
9. PERFORMING ORGANIZATION NAME AND ADDRESS Battelle-Columbus Laboratories 505 King Avenue Columbus, Ohio 43201		10. PROGRAM ELEMENT, PROJECT, TASK AREA & WORK UNIT NUMBERS 61102F 2306/A1
11. CONTROLLING OFFICE NAME AND ADDRESS Air Force Office of Scientific Research/NE Bldg. 410, Bolling AFB, D.C. 20332		12. REPORT DATE February 28, 1979
		13. NUMBER OF PAGES 56
14. MONITORING AGENCY NAME & ADDRESS(if different from Controlling Office)		15. SECURITY CLASS. (of this report) Unclassified
		15a. DECLASSIFICATION/DOWNGRADING SCHEDULE

16. DISTRIBUTION STATEMENT (of this Report)

Approved for public release; distribution unlimited.

17. DISTRIBUTION STATEMENT (of the abstract entered in Block 20, if different from Report)

18. SUPPLEMENTARY NOTES

19. KEY WORDS (Continue on reverse side if necessary and identify by block number)

Forging   Nickel
Extrusion Forging   Workability
Ring Forging   Hot Working
Aluminum

20. ABSTRACT (Continue on reverse side if necessary and identify by block number)

A combined metallurgical and mechanical study of hot forging is described. Theoretical predictions of strain and temperature distributions are compared with experimental observations for both ring and extrusion forgings. It is shown that a complete description of the process requires understanding of friction, heat flow, constitutive behavior (including both deformation and fracture), and of the basic equations of continuum mechanics. To a large extent the predictions agree with experiment although differences

TABLE OF CONTENTS

⑨ FINAL TECHNICAL REPORT, *1 Jan 76 - 31 Dec 78*,

on

⑥ EFFECTS OF HOT FORGING VARIABLES UPON MICROSTRUCTURE
AND PROPERTIES OF METALS AND ALLOYS,

(Grant No. AFOSR-76-2971)

⑮ to

AIR FORCE OFFICE OF SCIENTIFIC RESEARCH

by

⑩ T. Altan*, A. H. Clauer, G. D. Lahoti,
A. R. Rosenfield*, and T. L. Subramanian

from

BATTELLE
Columbus Laboratories

⑪ 23 Feb 79   ⑫ 59 p.

1. INTRODUCTION   ⑱ AFOSR

⑯ 2306   ⑰ A1   ⑲ TR-79-0239

1.1. Program Organization

The objectives of this program were to develop a fundamental
understanding of hot forging by showing how complex strain, time, tempera-
ture histories affect the material response. The research combined the
contributions of several engineering disciplines, including materials
science, mechanics of large deformations, heat transfer, and interface
effects. To achieve its objectives, the project was conducted at Battelle-
Columbus Laboratories by the staff of Metalworking and Metal Science
Sections. Dr. Taylan Altan (Metalworking) and Dr. A. R. Rosenfield (Metal
Science) were co-principal investigators. In addition to Dr. Altan,
Drs. T. L. Subramanian and G. D. Lahoti participated in the mechanics
phase while Dr. Rosenfield and Dr. A. H. Clauer cooperated in the materials
phases.

---

*Principal Investigator.

In one sense the program organization itself was experimental, since the researchers had to develop ways to combine their differing approaches to the problem. These approaches involved not only the different perspectives of experiment and analysis but also both continuum and micro-structural viewpoints. The complete integration of all these elements into a unified approach to an exceedingly complex problem proved to be difficult. However, the program goals were substantially attained.

1.2. Coupling

This project was successful in identifying and evaluating the detailed information necessary for the combined materials and mechanics study of metal processing problems. The research and the coupling efforts conducted during this program led to the formulation and organization of a larger basic study on "Research to Develop Process Models for Producing a Dual Property Titanium Alloy Compressor Disk". This new program is sponsored by the Metals and Ceramics Division of AFML with Dr. Harold Gegel as project manager. Battelle-Columbus is prime contractor of this new program and has the following subcontractors:

  (1) University of California, Berkeley (S. Kobayashi)

  (2) Wright State University (J. Thomas)

  (3) Los Alamos Scientific Laboratory (J. Hockett)

  (4) University of Pittsburgh (H. Kuhn)

  (5) Wyman-Gordon Company (C. Chen).

Drs. T. Altan and G. D. Lahoti of Battelle-Columbus are directing the research on behalf of AFML.

1.3. Publications

The results of this program are to be reported in detail in seven publications. The first two, which have already appeared in the open litera-ture, are summarized in this report. The research leading to the other papers is described in greater detail herein. The publications are:

  (1) Nagpal, V., Lahoti, G. D., and Altan, T., "A Numerical
       Method for Simultaneous Prediction of Metal Flow and
       Temperatures in Upset Forging of Rings", published in
       ASME Transactions, J. Engr. Ind., November 1978, p. 413.

(2) Rosenfield, A. R., "Diametrical Compression of Rings", Strain, Vol. 14 (1978), p. 150.

(3) Altan, T., Lahoti, G. D., and Nagpal, V., "Systems Approach in Massive Forming and Application to Modeling of Forging Processes", accepted for publication by ASM Journal of Applied Metalworking.

(4) Lahoti, G. D., Nagpal, V., and Altan, T., "Selection of Lubricants in Hot Forging and Extrusion" presented at the Conference on "Lubrication Challenges in Metalworking and Processing", IITRI, Chicago, June 1978, and published in the Proceedings of the meeting.

(5) Subramanian, T. L., Lahoti, G. D., and Altan, T., Computer Simulation of Metal Flow and Prediction of Process Variables in Extrusion-Forging", in preparation for submission to ASME Transactions.

(6) Rosenfield, A. R., "Environmentally-Assisted High-Temperature Fracture of Nickel", in preparation for submission to Metallurgical Transactions.

(7) Clauer, A. H., and Lahoti, G. D., "Microstructural Analysis of Extrusion Forgings", in preparation.
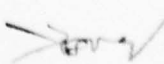
2. BACKGROUND

Most metal and alloy parts are hot-worked at some point during processing to produce flaw-free components having uniform composition and microstructure: a microstructure suitable for subsequent solution, stabilizing, and aging treatments. Ideally, the condition of the as-worked alloy should allow it to be heat treated so as to produce optimum combinations of strength and toughness. Some metals and alloys, such as aluminum and ferritic steels, are relatively easy to hot work. Others, such as the high temperature superalloys and titanium alloys are more difficult to fabricate since they were designed to resist high temperature deformation. The alloy additions and precipitates introduced to enhance the high temperature strength also combine to raise the flow stress, decrease ductility, and restrict the temperature range for hot-working.

This research program focused on hot forging of nickel. Nickel-base alloys, their development, and fabrication are important to the Air Force in its efforts to increase the operating temperatures, decrease weight in aircraft, and to minimize waste during processing to the final products. Hot forging is an important step in the forming of engine discs, blades and vanes of superalloys or titanium alloys, and also in forming non-engine components such as aluminum or titanium alloy structural air-frame parts. Accordingly, a basic understanding of the hot forging process is important for improving its efficiency and usefulness.

As alloys grow more complex, hot workability and the determination of the parameters yielding suitable uniformity of composition and microstructure in a sound part tend to become more difficult and costly, expecially when done largely by full-scale empirical methods. Because of this, it is desirable to develop alternative methods or models to evaluate different hot working parameters. Such models should be based both on an understanding of the mechanisms of hot working and the variation of the process variables throughout the part during hot-working.

This kind of research can best be accomplished through an approach incorporating a cooperative interaction between materials scientists engaged in high temperature deformation and fracture, and mechanicists experienced in analyzing metal flow during complex processing operations. This grant

combined both approaches in an interactive manner to selected metals
alloys. The goal was to further the fundamental understanding of the
mechanisms of hot working including flow and fracture, to analyze in
detail the hot forging process for several simple shapes, and to tie these
areas together in an analysis of the relation between the hot forging
parameters and the material response in terms of microstructure, cracking,
working loads, and temperatures.

The technical work was specifically concentrated on developing a
process model for an extrusion-forging process using (a) pure aluminum
(Al 1100) and (b) commercial purity nickel (Ni-270) as the materials under
investigation. The study was aimed to cover (a) the characterization of
the basic material response (e.g. flow and fracture), (b) the characteriza-
tion of process variables (temperature, interface conditions, deformation
rate, die geometry), (c) the relation between material and process
variables, and (d) the development of relations between process conditions
and microstructure.

The general approach to the problem is outlined in Figure 2.1,
which is a schematic plan in the form of a flow chart. The chart shows
that the approach contains both experimental and theoretical parts.
Initially experiments were used to define the flow and fracture properties.
The appropriate mathematical relations to describe the relations between
process variables and material response were then formulated. Outputs
from both of these approaches were combined into a computer-based process
model. The same conditions were then applied to a laboratory-scale
extrusion forging. Finally, the results of the computer study were compared
to the parameters of the actual forging, particularly with respect to local
strain distribution.

This report describes the progress made within the framework out-
lined in the above paragraph. Initially, the separate input phases are
discussed: Section 3 describes the experiments to define the flow behavior
while Section 4 describes the approach adopted to characterize crack
formation and growth. Section 5 concentrates on the development of the
computer process model and includes some exploratory experiments on ring
forgings. Section 6 is a discussion of the experimental and analytical
results obtained on the extrusion forging. Finally, Section 7 offers
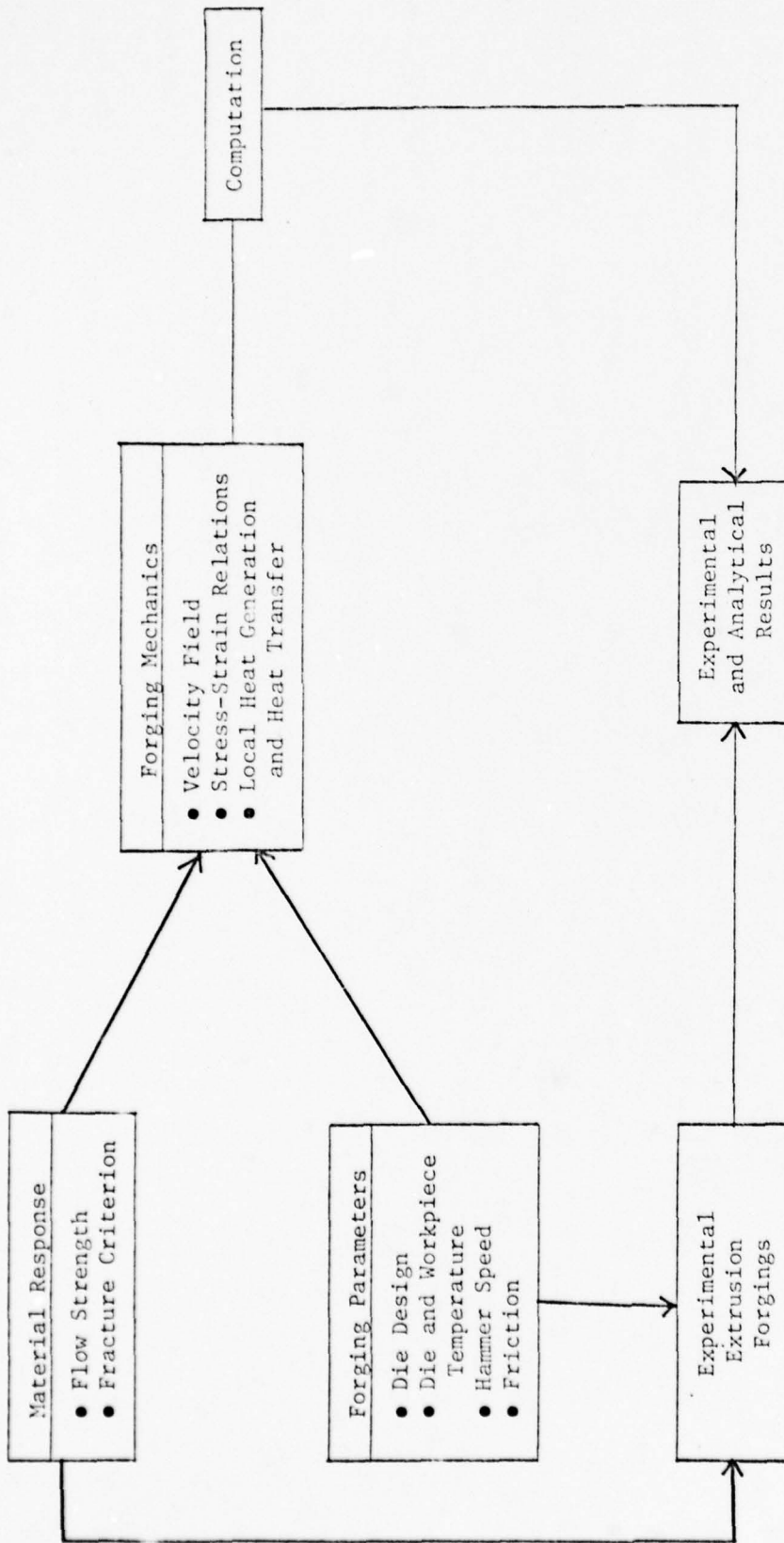some conclusions.

FIGURE 2.1. SCHEMATIC FLOW CHART OF THE RESEARCH PLAN FOR AN INTEGRATED MATERIALS/MECHANICS STUDY OF HOT FORGING

The research approach described in this report has broad general applicability. In fact, this research approach, i.e., investigation of a deformation process from both materials science and mechanics point of views, emphasized in this program, lead to the large basic research study on "Developing Process Models for Producing a Dual Property Titanium Alloy Compressor Disk". This program is now being sponsored by the Metals and Ceramics Division of AFML and is being conducted by Battelle-Columbus and several subcontractors.

3. HIGH TEMPERATURE FLOW AND MICROSTRUCTURE

The objective of this phase was two fold, both to generate flow property data which could be used as material property input for the computer analysis of the forging process and to establish the relation between microstructure and hot deformation under simple upset compression which could then be used to study the microstructures developed in more complex forgings. The dependence of the microstructural changes on deformation temperature, strain rate, total strain, and time at temperature was to be determined under isothermal uniaxial deformation conditions. This microstructural dependence would then be used to characterize deformation/ temperature histories, in a complex forging shape.

The approach for the microstructural analysis was to use in-material changes, observable after hot working and sensitive to local deformation conditions of strain, strain rate and temperature, to correlate the microstructures in complex forgings with the internal distributions of strain, strain rate and temperature predicted by the computer analysis. The microstructural parameter selected for the initial experiments was the subgrain size in pure aluminum. Extensive previous research had shown that the subgrain diameter developed during hot deformation of aluminum correlates to the flow stress and, through the Zener-Hollomon parameter, also to the strain rate, and temperature (McQueen and Hockett, 1970). Aluminum was a desirable material for the initial studies because large specimens could be forged for analysis without overloading the laboratory press, and in addition, it does not recrystallize easily, enabling the subgrain size to be evaluated over a large range of strain and temperature.

The microstructural parameter selected for the experiments on nickel was the grain size. Previous research on recrystallization of nickel during hot working showed that dynamic recrystallization occurred during hot working after a certain critical strain was reached (Luton and Sellars, 1969). In addition, the critical strain necessary for dynamic recrystallization is dependent on strain rate, temperature and flow stress. Finally, the recrystallized grain size was dependent on the flow strength, independent of temperature. Thus, in principle, for appropriate selection of the forging conditions, the boundaries between recrystallized and unrecrystallized regions could be related to calibrated values of strain,

strain rate, and temperature, while relative grain size might indicate relative stress levels.

The important results of these investigations are presented next.

3.1. Aluminum

The material for this phase of the program was 1100-F aluminum (99.0% minimum purity) obtained in the form of 100 mm diameter bar. Because of the requirement that the subgrain size reflect the hot working conditions being studied, it was imperative to either remove all subgrain boundaries or to make them much larger than the largest size to be reached in the experiments. It was intended to heat treat the material, induce recrystallization and grain growth, and "sweep up" the subgrains.

Annealing the as-received wrought bar at temperatures to 625 C (0.96 Tm) caused some grain growth and relaxation of the dislocations in the subboundaries, but not enough to be suitable for the purpose of this program. In an effort to induce recrystallization and thereby remove the substructure, the rod was cold rolled in increments down to 75 percent reduction and slices were annealed at 350, 400, 450, and 500 C. Recrystallization occurred in most cases, but the grain sizes were quite small and the substructure had not been removed. Duplex anneals, recrystallization at a lower temperature and grain growth at higher temperature, were also carried out. Recrystallization had clearly occurred after 50 and 75 percent reduction plus anneals but transmission electron microscopy showed subgrains still present within the grains with a diameter of about 1 μm. This subgrain size is at the lower end of the size range for our purpose. Long time anneals to foster grain growth were no more successful.

An alternative approach was then tried based on the inverse relation between subgrain size and creep stress. By using low stresses and high temperatures it was intended that low stress creep deformation would considerably expand the size of the subgrains. To this end, a recrystallized specimen was annealed at 649 C (0.98 T_m) under a stress of 0.1 MPa, producing in effect a stress-induced recovery process. This procedure should have produced a subgrain size of the order of a millimeter in diameter (McQueen and Hockett, 1970). Transmission microscopy of the specimen after

creep showed slightly enlarged subgrains with somewhat unraveled boundaries. This too was not satisfactory for the purpose of the problem.

Among the causes of this difficulty in removing the subgrains were (i) large cold work strains were required to work the entire cross section of the large bar. This decreases the recrystalline grain size. (ii) there were sufficient impurities and oxide particles (observed by TEM) to inhibit the grain growth needed to sweep up the subgrains, and (iii) aluminum is more prone to recovery which limits the driving force for recrystallization and grain growth. On the basis of these unsuccessful attempts to obtain a starting microstructure suitable for the intended experiments, the experiments on aluminum were discontinued.

3.2. Nickel

The desired starting microstructure for the nickel was a relatively large, equiaxed grain size such that recrystallized areas would be easily seen and a wide range of recrystallized grain sizes would be distinguishable from the starting microstructure. After a number of trials, a relatively large grain size averaging 0.18 mm diameter* was obtained by hot forging and swaging the as-received bar followed by a two stage anneal consisting of 1 hour at 700 C followed by 0.5 hour at 927 C.

Isothermal upset compression tests were performed at 700 to 1100 C with most of them being in the range 700 to 900 C. The nominal range of strain rate covered was 1 to 25 sec^{-1} to final true strains of 0.1 to 0.8. The flow stress data were obtained by computer digitizing the load-time data for each specimen and converting them to true-stress/true-strain and true strain/true-strain-rate curves.

Immediately after upset compression (in a jig heated to the deformation temperature to maintain isothermal forging conditions) the specimens were quenched into cold water to stop recrystallization and grain growth. The time before quenching was recorded for each test, averaging about 8 seconds. Duplicate specimens held for 30 seconds before quenching showed no grain size differences compared to the more rapidly quenched specimens. Therefore, any rapid transients in recrystallization and grain growth occurred within the 8 second interval.

---

* The grain sizes are all given as the average linear intercept distance.

3.2.1. Flow Properties

The flow properties obtained from both the digitized upset compression data and calculated from the side pressing of the rings in the workability experiments (see Section 4) are shown in Figure 3.1. The solid curve is taken from Luton and Sellars (1969) and shows very good agreement with the side pressing experiments but less agreement with the upset compression results. This is because the side pressing experiments were performed at lower strain rates and the saturation stresses were reached at low strains during the tests. The upset compression data were performed at the highest strain rates, and in most cases did not reach the saturation flow stress within the 0.4 to 0.8 true strain range possible for these tests. Therefore the flow stress data tend to show lower flow stresses than predicted by the solid curve. This is no problem for the computer analysis of the upset compression and forging process, since the analyses use the actual true stress-true strain curves for the calculations rather than the steady state flow properties. These true stress-true strain curves were obtained by digitizing the load and deflection curves. Typical curves are shown in Figure 3.2.

3.2.2. Microstructure

Each of the upset compression specimens was sectioned longitudinally and the grain size was measured at six locations along the center diameter and along the vertical axis of each specimen. This provided a determination of the grain size distribution within the specimens, to compare with the strain distribution predicted by the computer code, and an overall measurement to correlate with the strain, strain rate, and temperature conditions of all the tests.

The overall dependence of post-compression grain size on the total strain, strain rate, temperature conditions was so uneven that no useful correlations could be drawn from these data. The data at 700 C were the best although they had a wide scatter band. They showed a decreasing grain size with increasing strain (Figure 3.3). The correlation of critical strain versus strain rate conditions for onset of dynamic recrystallization was reported by Luton and Sellars (1969) could not be clearly discerned in these experiments. It is possible that metadynamic recrystallization and
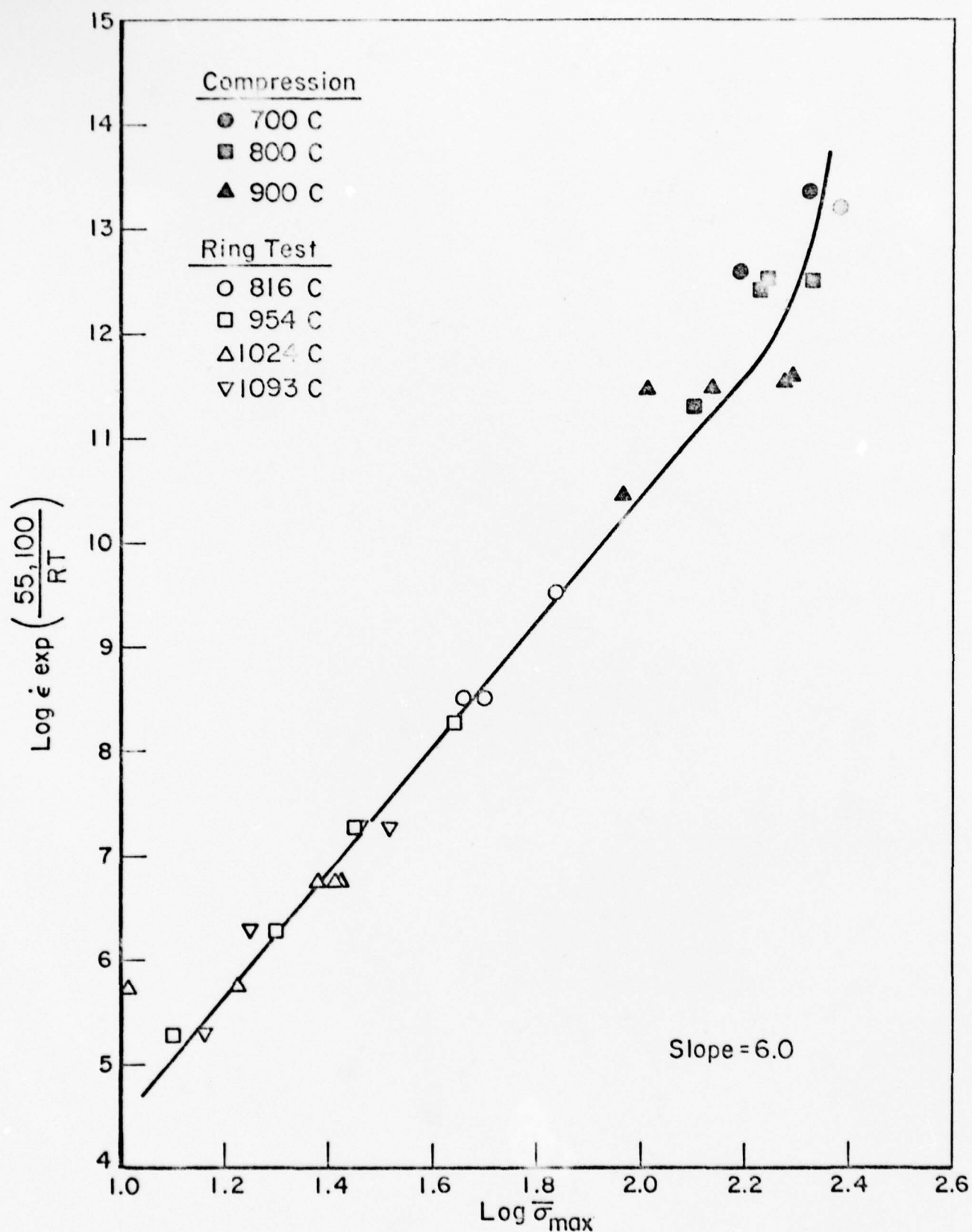
FIGURE 3.1. FLOW BEHAVIOR OF NICKEL FROM BOTH THE UPSET COMPRESSION TESTS AND THE SIDE BENDING OF RINGS TEST

The maximum flow stress is plotted versus the true strain rate at the maximum stress. The solid line is from Luton and Sellars (1969).
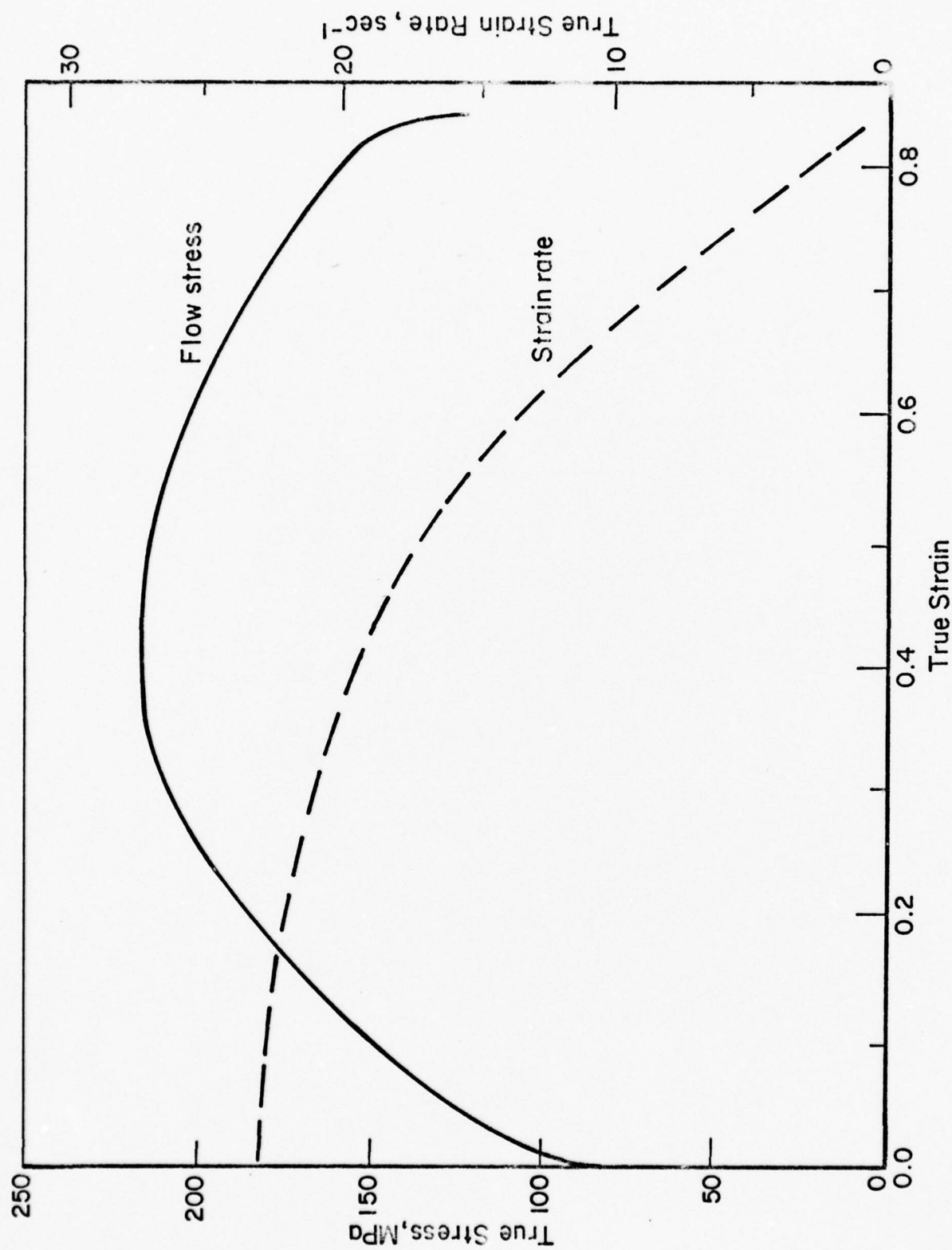
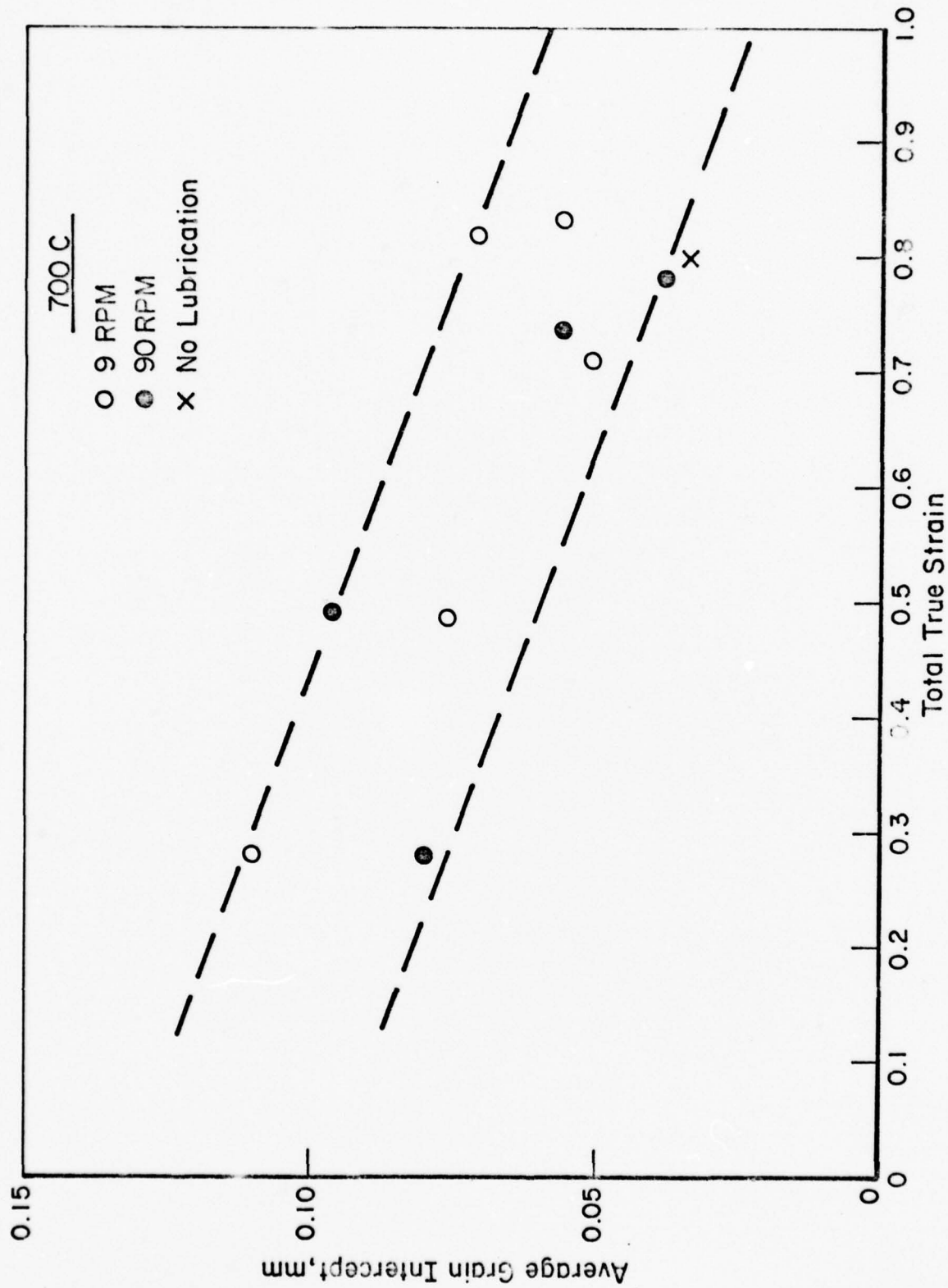FIGURE 3.2. TYPICAL TRUE STRESS AND TRUE STRAIN RATE VERSUS STRAIN CURVES FOR UPSET COMPRESSION OF NICKEL

FIGURE 3.3. VARIATION OF GRAIN SIZE IN CENTER OF NICKEL UPSET COMPRESSION SPECIMENS WITH
TOTAL STRAIN AND STRAIN RATE AT 700 C

15

grain growth subsequent to the compression tests washed out this correlation. This was not expected because their reported time before quenching was about 5 seconds and in this study it was 8 to 15 seconds with no effect of increasing the time to 30 seconds.

Although no quantitative correlation of grain microstructure with local deformation conditions can be made, it is possible to see non-uniformities in the deformation within an upset specimen or forging by the non-uniformity in grain size. Virtually all the upset compression specimens in which the grain size distribution was measured (42 specimens) showed the same pattern. The grain size in the center of the specimens was smaller than elsewhere. Typical examples are shown in Figures 3.4 and 3.5, wherein the measured average grain intercept is indicated on longitudinal sections of the specimens in Figures 3.4a and 3.5a and the computer predicted strain distribution is shown in Figures 3.4b and 3.5b. The predicted strain distribution is quite uniform. The predicted temperature distribution in each case was also quite uniform. At 700 C, the specimen temperature was 718 to 722 C and at 800 C the specimen temperature was 818 to 821.5 C with the temperature decreasing from the center to the ends of the specimens.

There are several possible combinations of strain, strain rate and temperature which could cause the observed variation in grain size within the specimens and these cannot be differentiated here. If there is a decrease in grain size with increasing total strain (Figure 3.3), then the microstructural results (Figures 3.4a and 3.5a) suggest that the strain is largest in the center of the compression specimens. This is similar to what was predicted by Kobayashi, Lee and Oh (1973) for upset compression of steel. In the present investigation, a more approximate method, namely, the upper-bound method, was utilized to predict metal flow. Although this method of anlysis is capable of predicting the overall deformation fairly accurately, the strain distribution can be predicted only approximately. This is due to the fact that the assumed velocity distribution itself is approximate in nature, and it does not include bending of radial flow lines and folding of free surfaces. Further, this method assumes that the entire metal under the dies undergoes plastic deformation and neglects formation of dead-metal zones near the die-workpiece interfaces.
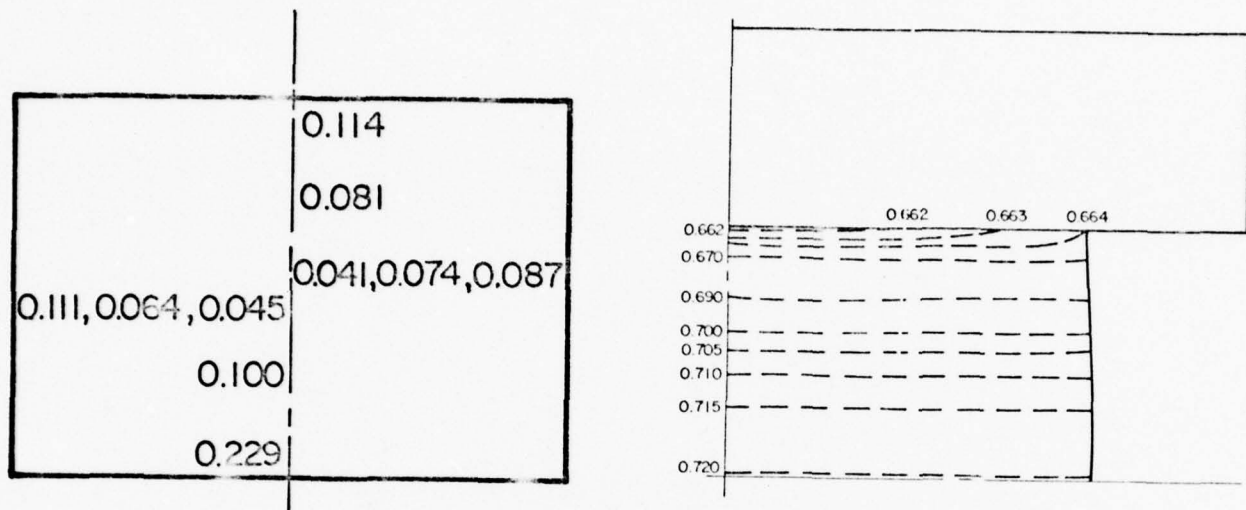
a. Grain size distribution over entire specimen cross section

b. Calculated strain distribution over upper right quadrant of specimen.

FIGURE 3.4. COMPARISON OF THE GRAIN SIZE DISTRIBUTION AND STRAIN DISTRIBUTION OVER A LONGITUDINAL SECTION THROUGH A SPECIMEN UPSET AT 700 C AND 13.8 sec^{-1} INITIAL TRUE STRAIN RATE TO 0.737 TOTAL TRUE STRAIN

The upset direction is vertical.
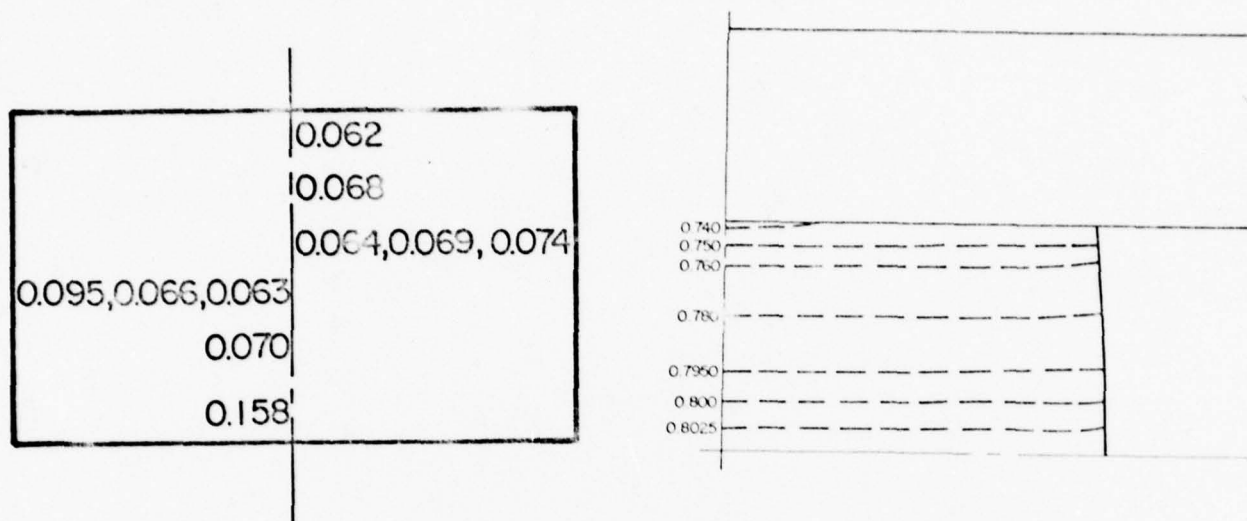
a. Grain size distribution over
    entire longitudinal section.

b. Calculated strain distribution
    over upper right quadrant of
    specimen.

FIGURE 3.5. COMPARISON OF THE GRAIN SIZE DISTRIBUTION AND STRAIN DISTRIBUTION
OVER A LONGITUDINAL SECTION THROUGH A SPECIMEN UPSET AT 800 C AND
23.4 sec^{-1} INITIAL TRUE STRAIN RATE TO 0.805 TOTAL TRUE STRAIN.

The upset direction is vertical.

Several non-isothermal forging conditions were also studied. To make the deformation non-uniform, cold, non-lubricated dies were used. The resulting microstructures were very non-uniform, showing evidence of high strain shear bands diagonally across the specimen as seen in Figure 3.6c as the very fine grained recrystallized regions. The predicted temperature and strain distributions are shown in Figures 3.6a and b. The flow stress data used for the lower temperature regions in these calculations were extrapolated from the higher temperature data of this study. Again, the predicted strain distributions are much more uniform than the microstructure would suggest.
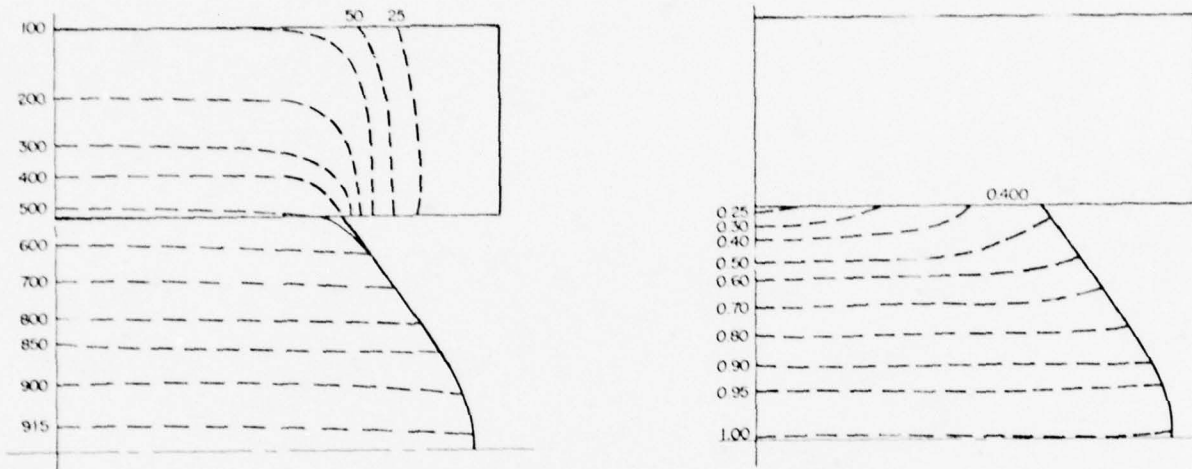
a. Temperature distribution.

b. Strain distribution.

c. Microstructure.

FIGURE 3.6. COMPARISON OF PREDICTED TEMPERATURE AND STRAIN DISTRIBU-
TION TO THE ACTUAL MICROSTRUCTURE OF A SPECIMEN UPSET
UNDER COLD DIE, NO LUBRICATION CONDITIONS TO CREATE NON-
UNIFORM FLOW

The specimen was upset at 900 C and 23.8 sec^{-1} initial
strain rate to 0.781 total true strain. The upset
direction is vertical.

4. WORKABILITY

The object of the workability phase of the research was to determine the maximum possible severity of strains which could be tolerated in the extrusion forging. To do so it is not only necessary to have a failure criterion which expresses fracture strain in terms of process variables (such as stress, strain rate, and temperature), but which also accounts for how the largest principal strain at fracture varies with other components of the strain tensor.

At the outset of the program, we were faced with two major problems in specifying hot workability of nickel:

(1) There was no standard workability test method, and

(2) There was no method of extrapolating data from one stress system to another.

A third problem was that almost all of the fracture data reported in the literature were obtained in inert atmospheres, while hot working operations are carried out in air.

Some guidance existed on the question of the stress system effect. Ongoing research at Battelle-Columbus (Lahoti, et al., in press) had suggested that the surface fracture criterion (Lee and Kuhn 1973) is valid at high temperature and Kuhn and Dieter (1977) published confirmatory data during the course of the grant. According to this approach:

$$\varepsilon_T = \varepsilon_{ps} + 1/2 \left| \varepsilon_c \right| \tag{4.1}$$

where ε_T and ε_c are principal strains parallel to the surface and ε_{ps} is the plane strain ductility. The implication of Equation (4.1) is that ε_{ps} is the basic material property describing resistance to crack formation. The experimental problem then became one of measuring ε_{ps}.

Several years ago, Battelle-Columbus carried out research on an Air Force project involving ambient temperature fracture of high strength aerospace alloys (Hahn, et al., 1975). This work involved three-point bending of alloy sheet specimens. While these experiments were successful

in revealing the microscopic failure mechanism, adaptation of the existing design to high temperature crack formation would have been a formideible problem since a precision loading apparatus would have to be machined from a ceramic.

Research under the subject grant initially focused on development of a method which would provide a direct measurement of plane-strain ductility. The requirement was for a simple specimen/loading-jig design the use of which would require a minimum of instrumentation. The solution adopted was the side-pressed ring. Figure 4.1 shows a sketch of this geometry and the associated load, displacement curve. A paper has been published (Rosenfield, 1978) describing development of this geometry as a candidate test for measurement of basic ductility. The major conclusions of the paper were:

(1) Plane-strain deformations up to 20% true strain can be achieved using the side-pressed ring.

(2) The maximum strain in the specimen is simply related to the crosshead displacement.

(3) As a side benefit, the flow strength can be reliably measured from the load/displacement curve.

Prior to embarking on experiments on this test geometry, it was decided to evaluate it by examining edge cracking in hot rolling of titanium alloys as part of a then-existent NSF grant. The final test of the method was successful (Lahoti, et al., in press).

To provide a workability criterion for extrusion pressed rings of nickel were fabricated and test conditions specified so that the workability experiments would cover a wide range of the parameter $z = \dot{\varepsilon} \exp (Q/RT)$, where ε is strain rate, Q is activation energy, and T is temperature. The nickel was from the same bar that was used for extrusion forgings and the same annealing procedures were used. All tests were carried out in air.

Rings were machined from commercial purity Ni (grade 270). Their dimensions were 25 mm O.D., 12.7 mm I.D., and 5.4 mm thickness. Shallow flats were ground off the outer diameter opposite one another to facilitate positioning in the test rig. The rings were diametrically compressed between alumina anvils placed inside a furnace mounted on an Instron test machine. Displacement rates were an experimental variable. Most experiments were carried to complete closure of the ring although some
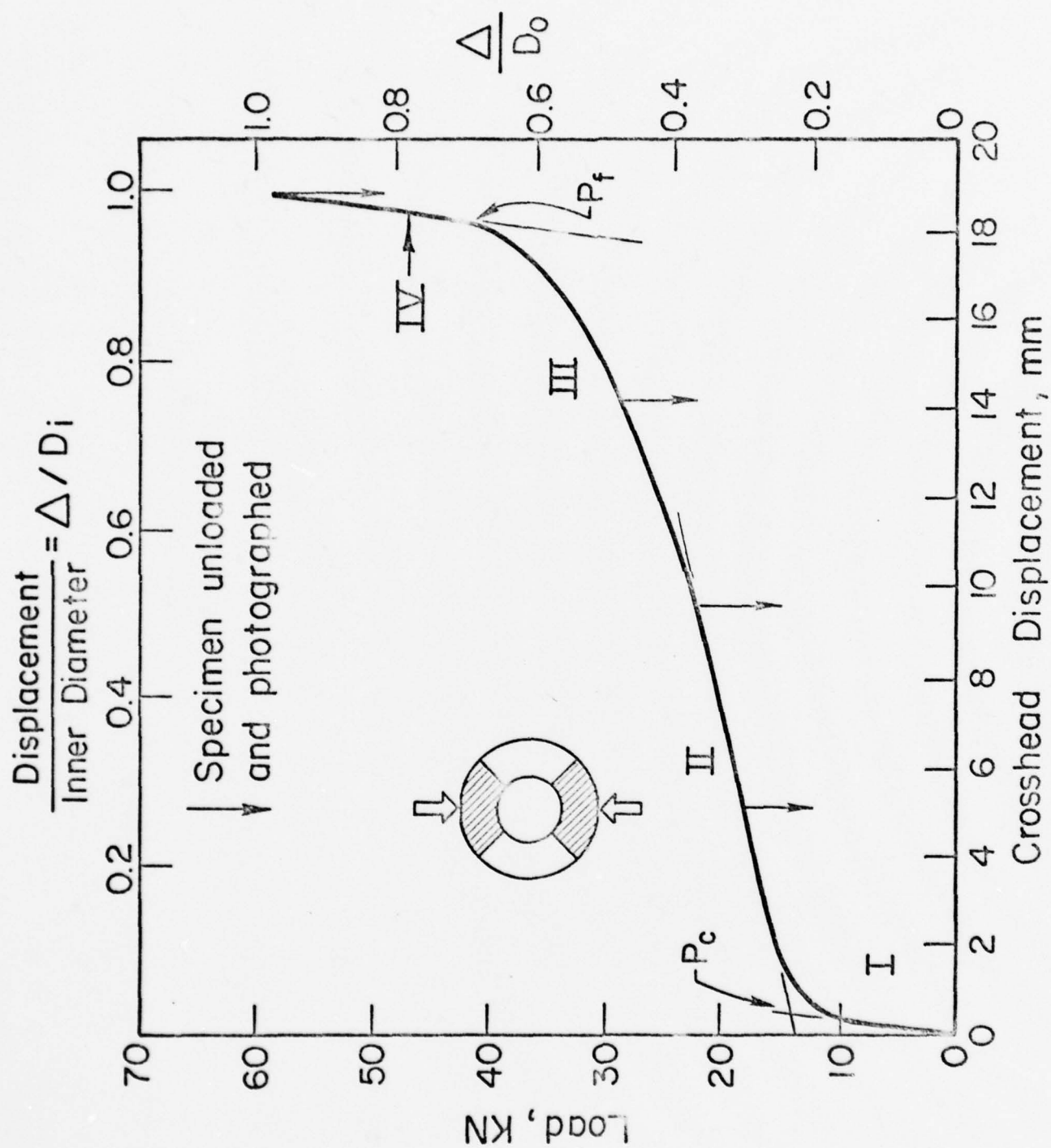
FIGURE 4.1.   LOAD/DISPLACEMENT RECORD FOR SIDE-PRESSED ALUMINUM RING TEST AT 23 C

were stopped short. In addition, some experiments were performed in which a 1.14 mm slot of 0.15 mm notch diameter was cut in order to study crack propagation. The slot extended from the inner rim and was aligned parallel to the loading direction.

Experiments were carried out over a range of temperatures between 816 and 1093 C and at strain rates between 3.22×10^{-5} and 3.22×10^{-2} sec^{-1}. Higher rates and lower temperatures were not examined since the range studied encompassed the crack/no-crack boundary for this geometry.

It was anticipated that crack formation would depend primarily on flow strength as was the case for the literature values reported for torsion specimens tested in inert atmosphere (Shapiro and Dieter, 1971). The strain for crack formation was large in specimens subjected to the high strain rates and low temperatures associated with high strength levels and small in specimens strained relatively slowly at high temperature. A similar effect was found in our experiments. Cracks initiated only in specimens tested so as to obtain lowest z values and specimens tested at the highest rates and lowest temperatures were crack free. However, a simple correlation between flow strength and crack initiation was not obtained. Instead, cracks were only found in specimens deformed above 1000 C. Furthermore, the cracks tended to be aligned parallel to the maximum normal stress (Figure 4.2) indicating that their formation was not dominated by shear, as might be expected if a flow process was involved. Furthermore, the crack pattern is suggestive of grain boundary failure.

Higher magnification microscopy, such as Figure 4.3, revealed that the grain boundaries were coated with an oxide layer. This observation is consistent with oxidation studies on stress-free nickel (Wood and Wright, 1965), where preferential grain boundary oxidation has been observed at temperatures over 1000 C. This leads to the following postulated model: initially, oxygen diffuses along the grain boundaries and either reduces grain boundary cohesion or reacts to form a brittle boundary layer; the layer breaks under the action of the tensile stresses exposing the grain boundary layer ahead of the crack tip to further oxidation. Accordingly, the process is autocatalytic.

An effort was made to measure crack propagation by side-pressing rings which contained narrow slits aligned normal to the tensile stress. As shown in Figure 4.4 this effort was unsuccessful in generating growth rate data, since a maze of cracks formed at the notch tip, not the single crack necessary for quantitative measurements.

FIGURE 4.2.   CRACK PATTERN OBSERVED IN
   THE TENSILE STRESS REGION OF THE SIDE-
   PRESSED RING

The ring was deformed to the point of
closure and the inner rim is at the
top of the picture. Maximum tensile
stress direction is horizontal.
Temperature = 1093 C.
Crosshead rate = 8.5×10^{-3} mm/sec.
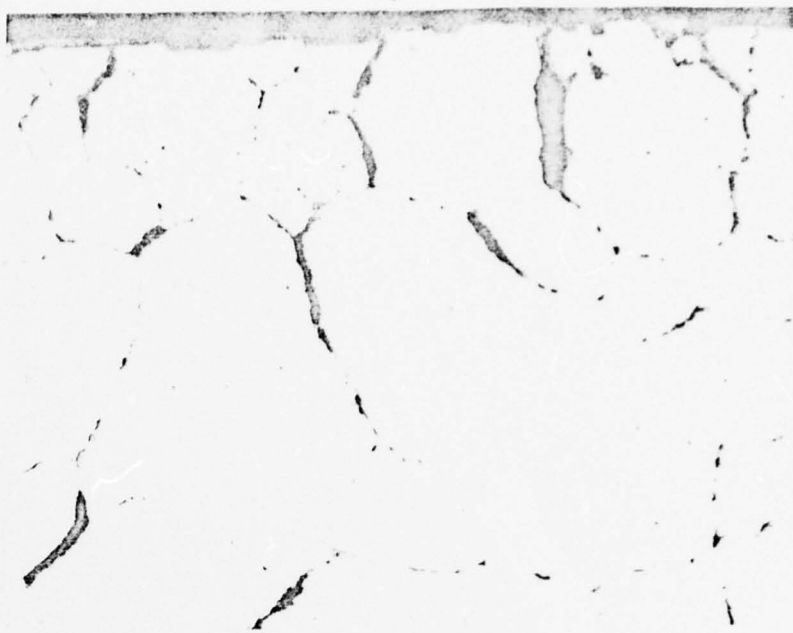Magnification 100X

FIGURE 4.3.   HIGHER MAGNIFICATION (500X)
   PHOTOMICROGRAPH OF SIDE-PRESSED RING
   DEFORMED UNDER THE SAME CONDITIONS
   AS THAT OF FIGURE 4.2.
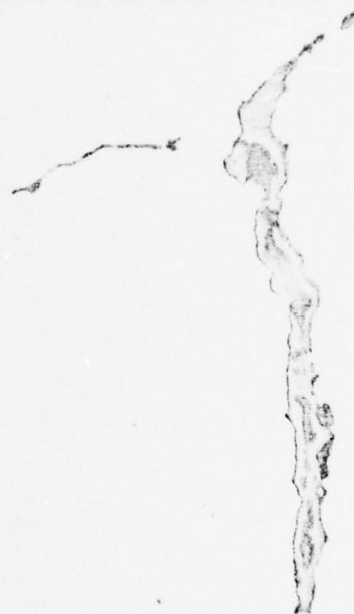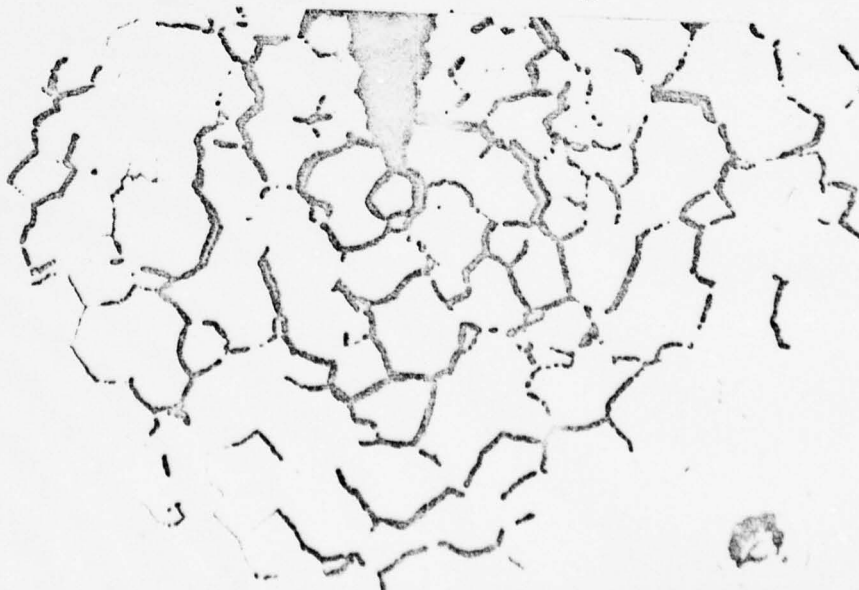
Oxide layer coats the rim of a crack.

FIGURE 4.4.   MAZE OF CRACKS
   SURROUNDING THE TIP OF A THIN
   SLOT WHICH HAD BEEN CUT INTO THE
   INNER RIM OF A SIDE-PRESSED RING

Test conditions and photomicro-
graph orientation as in Figures
4.2 and 4.3 (500X).

In conjunction with the literature, these results indicate that low strain fracture should not occur in the extrusion forging experiments provided the temperature is kept below 1000 C. For this reason a workability criterion was not included in the computerized process model. Support for this decision was provided by examination of extrusion forgings of nickel discussed below in Section 6. Figure 4.5 shows a fine crack pattern near a region of reentrant curvature. At higher magnification "fingers' containing corrosion products believed to be oxide are observed (Figure 4.6) as anticipated. Another high magnification photograph shows a typical region of cracking in greater detail and the pattern is reminiscent of those observed on the side-pressed ring. These observations suggest that rapid deformation can be carried out at 1000 C with very slight cracking problems. Further, the shallow depth of cracks in this extrusion forging suggests that the side-pressed ring provides a slightly conservative prediction of workability temperature.

The 900 C extrusion forging of nickel shows both apparent cracking and oxidation, but to an even lesser degree than at 1000 C. In this case the side-pressed ring experiments were slightly optimistic. However, the grain boundary oxidation mechanism appears to be operating.

In summary, the side-pressed ring test developed on this grant has been proven to be a useful new geometry for assessing strength and workability.

26

FIGURE 4.5. SURFACE CRACK PATTERN FORMED
IN AN EXTRUSION FORGING OF NICKEL

Forging temperature = 1000 C (100X).

FIGURE 4.6. LOCALIZED OXIDE GROWTH
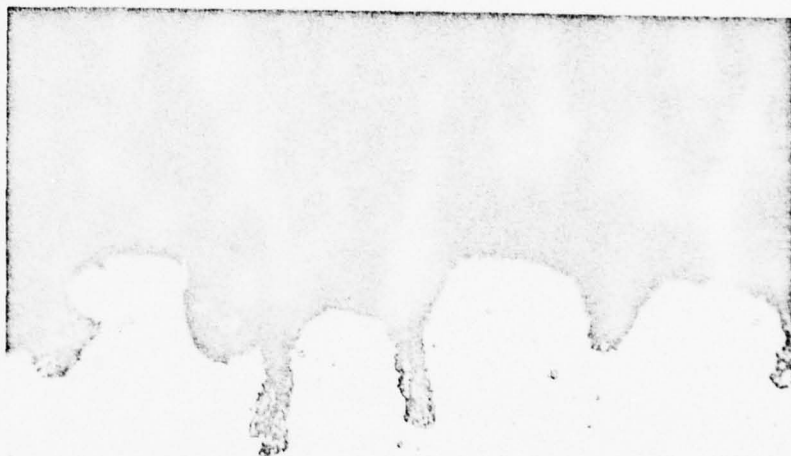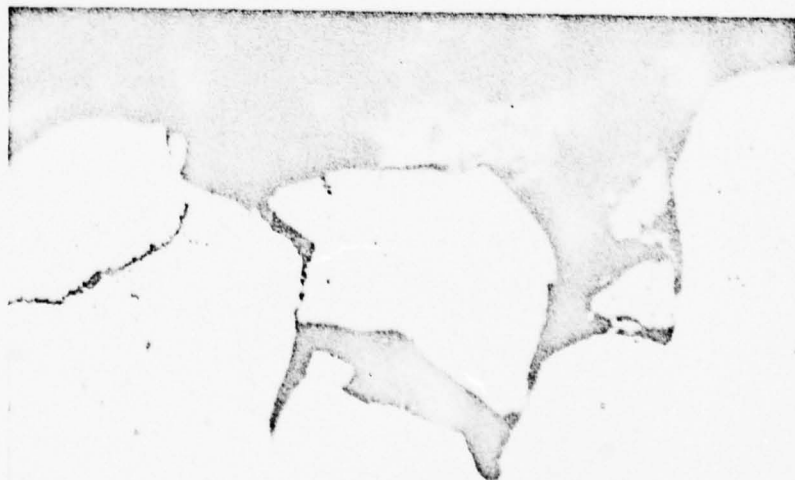NORMAL TO THE SURFACE IN THE SAME
FORGING (500X)

FIGURE 4.7. HIGHER MAGNIFICATION (500X)
PHOTOMICROGRAPH OF THE CRACK PATTERN
IN THE SAME REGION AS FIGURE 4.5

## 5. ANALYSIS OF METAL FLOW AND TEMPERATURES
IN UPSET FORGING OF RINGS

As a preliminary step to the analysis of extrusion forgings the simpler case of upset forging was considered first. This geometry is important in itself since upset of rings has been widely used as a test to characterize frictional conditions in forming processes and to evaluate lubricants (Schey, 1971; Speegelberg, et al., 1972). In this test, a flat ring-shaped specimen is forged to a known reduction between two flat dies. During forging, the internal diameter of the ring is reduced if the interface friction is high, and it is increased if this friction is low. Thus, the variation of the inside diameter of the ring during compression is a good indication of the frictional conditions at the tool-material interface.

Several mathematical analyses to predict metal flow in ring compression are available in the literature (e.g., De Pierre, et al., 1972; Lee and Altan, 1972; Lahoti and Kobayashi, 1974). However, none of these analyses includes the effects of strain rate and temperature distribution. Furthermore, these mathematical models assume a constant axial velocity on a plane perpendicular to the axis of compression. As a result, as shown in Figure 5.1a, all horizontal flow lines on a meridional plane remain striaght and parallel, even after considerable deformation under severe frictional constraints. Actual deformation patterns revealed by flow lines are shown in Figures 5.1b, 5.1c and 5.1d, where originally straight horizontal flow lines are curved after deformation. The folding of free surfaces is mainly due to this type of deformation. The ability to treat such distortion is important for the extrusion forging analysis described in the next section since nonplanar axial displacements are an important part of that process.

The ring forging analysis is described in detail by Nagpal, et al., 1977) and will be only briefly summarized here. In order to determine the velocity, strain rate and strain distribution in ring compression, the upper-bound velocity field by Lee and Altan (1972) was modified. In this velocity field, the axial component was considered as a function of both r and z (see Figure 5.1). The modified velocity field used here yielded a
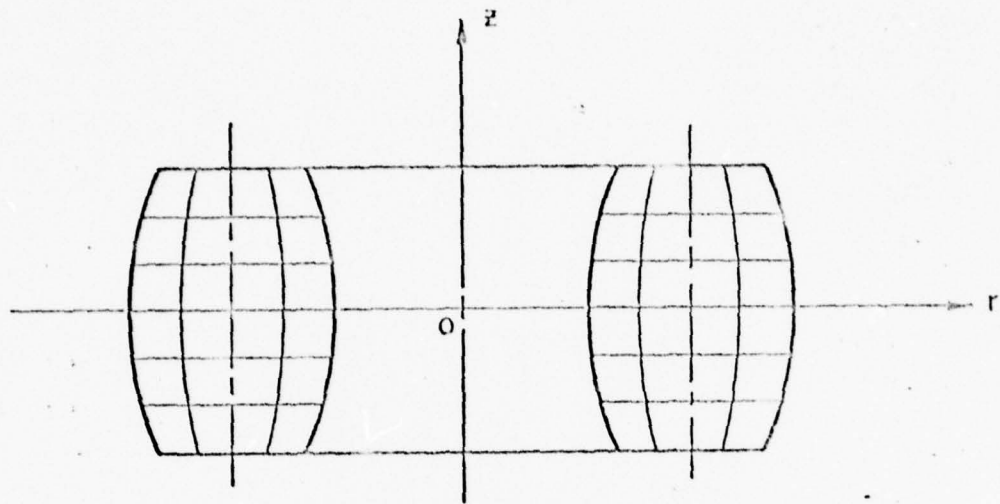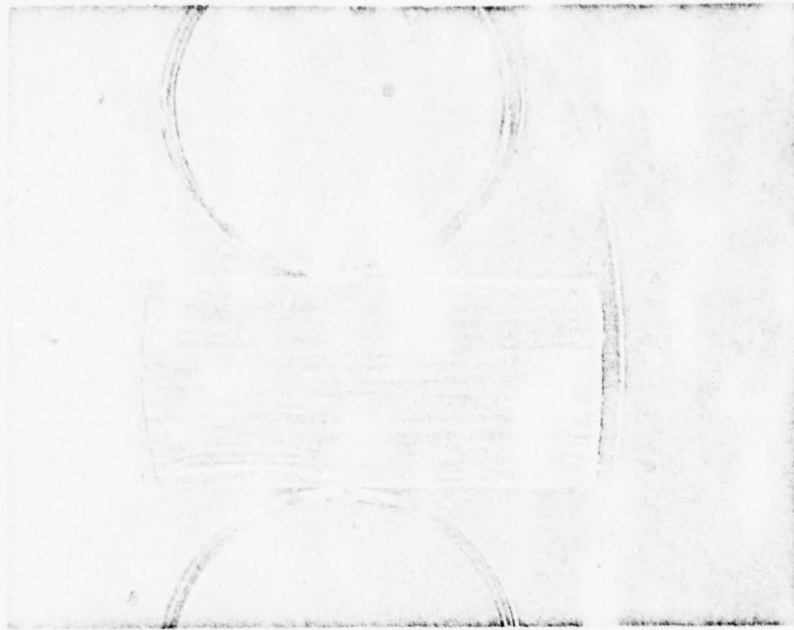
(a) Deformation Pattern Assumed in Existing
Analysis for Bulging
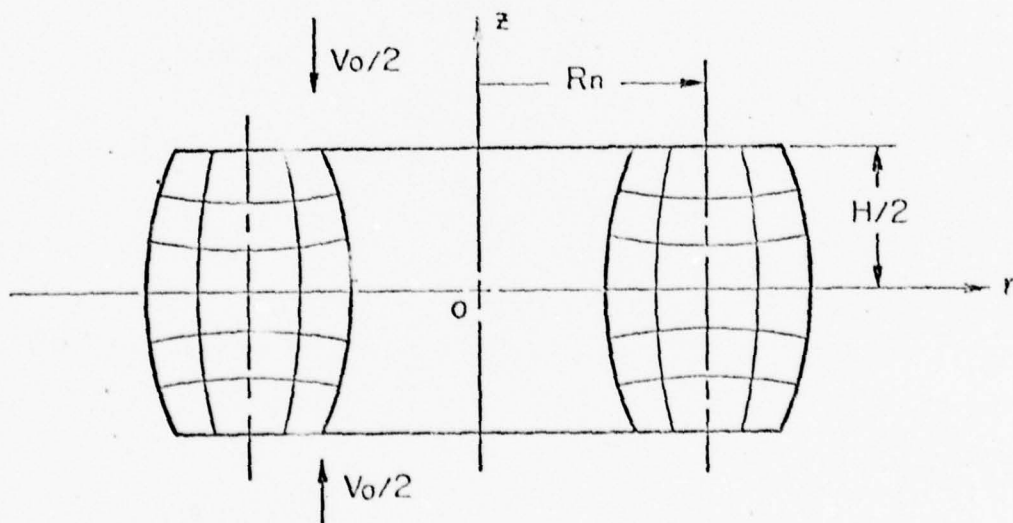
(b) Modified Deformation Pattern Assumed
in Current Analysis

FIGURE 5.1.

c. Flow patterns in aluminum ring compressed 30% at room temperature.

d. Flow patterns in an aluminum ring compressed 40% at room temperature.
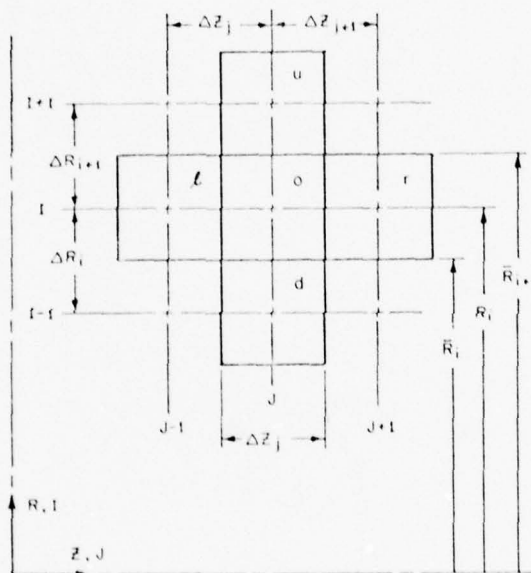
FIGURE 5.1.

FIGURE 5.2.   REPRESENTATION OF CYLINDRICAL GRID
SYSTEM FOR DERIVING THE DIFFERENCE
EQUATIONS OF HEAT CONDUCTION

lower value of the total energy rate compared to that of Lee and Altan's (1972) original velocity field. Therefore, according to the upper-bound theorem, the modified velocity field approximates the actual deformation more closely.

To predict the local temperatures during upset forging of rings, a well-proven finite-difference approach was utilized (Bishop, 1956; Lahoti, and Altan, 1975). For this purpose, the r-z plane of the ring was divided into a suitable orthogonal network, a cell of which is shown in Figure 5.2. The heat generation due to plastic deformation and friction is considered to take place at the beginning of a time interval Δt. The flow stress of an element of the deforming material is calculated for the temperature of the element in the preceding step, and the average strain and strain rate in the element calculated by the modified upper-bound technique (Lahoti and Altan, 1975).

5.1. Evaluation of Predicted Metal Flow and Temperatures

The modified analysis of metal flow and the analysis of temperatures in upset forging of rings were computerized in a program called RGTEMP. This computer program calculates the velocity, strain, strain rate and temperature distributions at each incremental reduction in the height of the ring. The total energy rate of the process, which is minimized using a numerical simplex method, and the forging loads are also calculated at each step of deformation.

To study the accuracy and limitations of the combined metal flow and temperature analysis, a limited number of aluminum 1100-F rings were upset forged in a mechanical press. The rings were upset forged between hardened-tool-steel flat, parallel dies at room temperature, and 427 C (800 F). The load-stroke curve was recorded on a light-beam oscillograph. In Figure 5.3, the theoretically predicted bulge profiles on the inside and outside free surfaces of the ring upset forged at room temperature are compared with experimental results. The edge of the predicted outside bulge surface does not agree very well due to the fact that this analysis does not consider folding of edges. Otherwise the comparison is reasonably good, considering that forged rings are not perfectly axisymmetric.
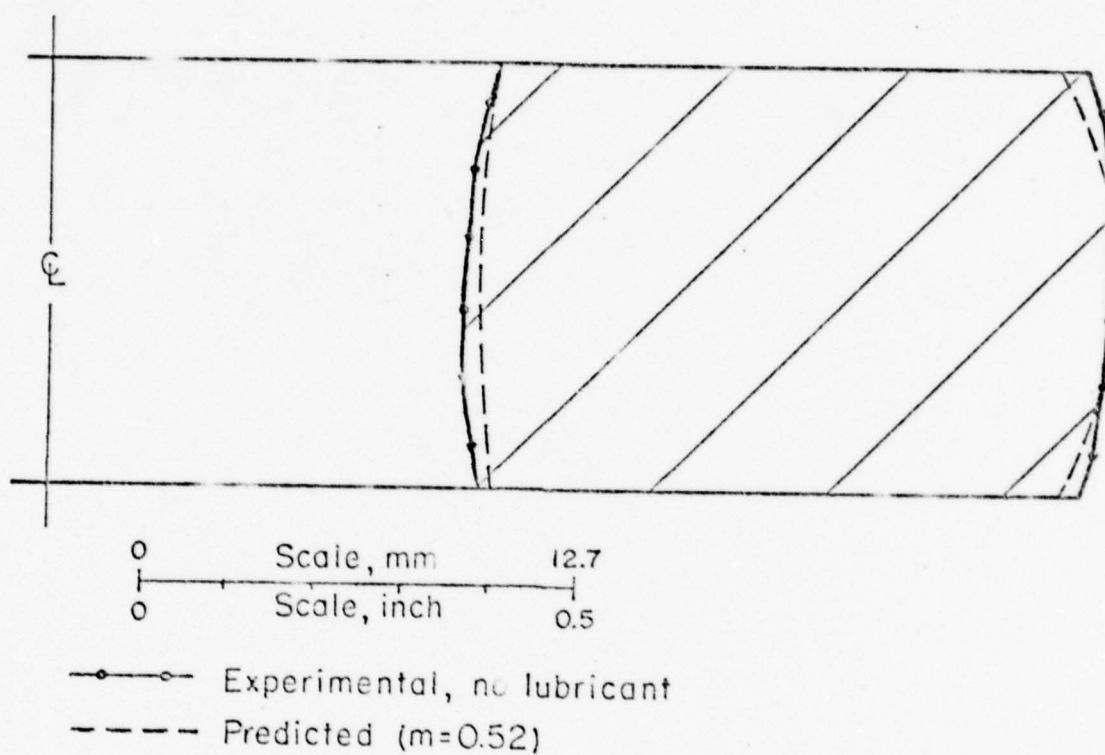
FIGURE 5.3. PREDICTED AND MEASURED BULGE PROFILES OF Al 1100 F RINGS UPSET FORGED AT ROOM TEMPERATURE TO 29.5 PERCENT REDUCTION IN HEIGHT

Pohl (1972) conducted an extensive study of the temperature distributions in cold upsetting of steel cylinders. In order to check the accuracy of the temperature analysis developed in the present study, predicted temperatures for a ring with very small holes were compared with Pohl's experimental data for a solid cylinder of identical dimensions. As seen in Figure 5.4, the predicted temperatures are in very good agreement with Pohl's thermocouple measurements.

5.2. Results of the Ring Analysis

This task on the analysis of metal flow and temperatures in ring compression resulted in a very significant contribution. The result of this task is a mathematical model and a computer program which predicts the metal flow in the ring test by taking into account the influence of the temperature gradients. It is the first time in metal deformation analysis that such a model, estimating simultaneously the temperatures and the flow, has been developed.

Additional conclusions reached in this task are:

(1) The previous method for simulating the ring compression test and the associated calibration curves for determining the friction shear factor m are not sufficiently accurate for estimating friction in hot forging when the interface friction is large (m > 0.5).

(2) The upper-bound velocity field, developed in this study, represents an improvement over most of the existing analyses of ring compression. However, this velocity field does not represent accurately the "folding of the edges", which occurs in upsetting under high friction conditions.

(3) The combined velocity-temperature analysis, developed in this study, is sufficiently accurate for estimating temperatures in hot and cold ring upsetting.

(4) The analysis of metal flow and temperatures, developed in this program is useful for investigating thermal effects in ring compression tests. This analysis is expected to improve the interpretation of experimental results of ring tests conducted at practical forging temperatures and under practical friction conditions (m < 0.5).
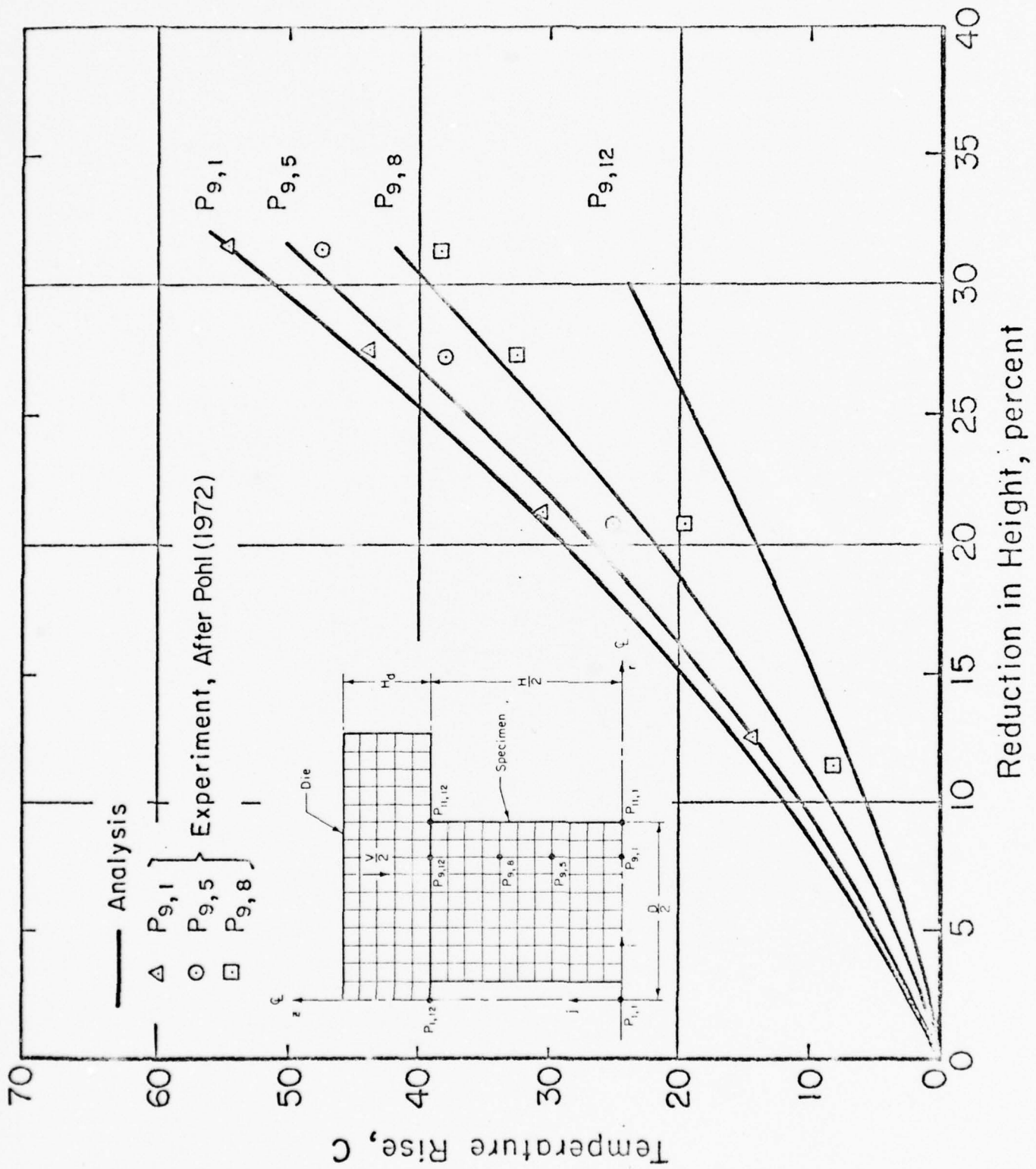
34

FIGURE 5.4. TEMPERATURE INCREASE VERSUS REDUCTION IN HEIGHT IN COMPRESSION OF RINGS

6. EXTRUSION FORGING

The objectives of this task were to develop an analysis of the metal flow and temperatures in the extrusion forging, shown in Figure 6.1 and to use microstructural changes as an aid in verifying the analysis.

6.1. Preliminary Metal Flow Experiments

In order to develop a reliable metal flow analysis from this complex geometry it was necessary to estimate the metal flow pattern in advance. For this purpose a limited number of preliminary extrusion forging experiments was conducted. Twenty specimens, 51 mm diameter by 57 mm high, were machined from Al-1100-F bar in as-received condition. These specimens were then heated at 400 C for 1 hour to obtain the annealed or 0-condition. Four additional specimens were machined from lead. The experimental tooling is shown in Figure 6.2. The upper and the lower dies were equipped with strip heaters to heat them up to 350 C.

The dies were mounted on Battelle's 500-ton mechanical press. A load cell was also placed between the top die and the top bolster plate. In order to protect the load cell from the hot top die, a water-cooled plate was inserted between the top die and the load cell. The load cell and an LVDT, mounted on the press ram, were connected to a light-beam oscillograph to record load and displacement individually with respect to time.

The lead specimens were forged at room temperature to 30, 45 and 60 percent nominal reductions in height with clean dies (without lubricant). The press speed was kept constant (90 strokes per minute) in all cases. An additional lead specimen was forged using dies lubricated with Fel-Pro C-300 lubricant. The four lead specimens after forging are shown in Figure 6.3.

Aluminum specimens were heated in an electric furnace to 315 and 425 C. The dies were heated to 315 C by strip heaters and gas flame on the die surface. Four specimens were forged to 15, 30, 45, and 60 percent nominal reductions in height at each temperature. At 425 C, the tests were repeated with dies coated with Fel-Pro C-300 lubricant. One set of aluminum specimens after forging is shown in Figure 6.4. In each case, the load and the press
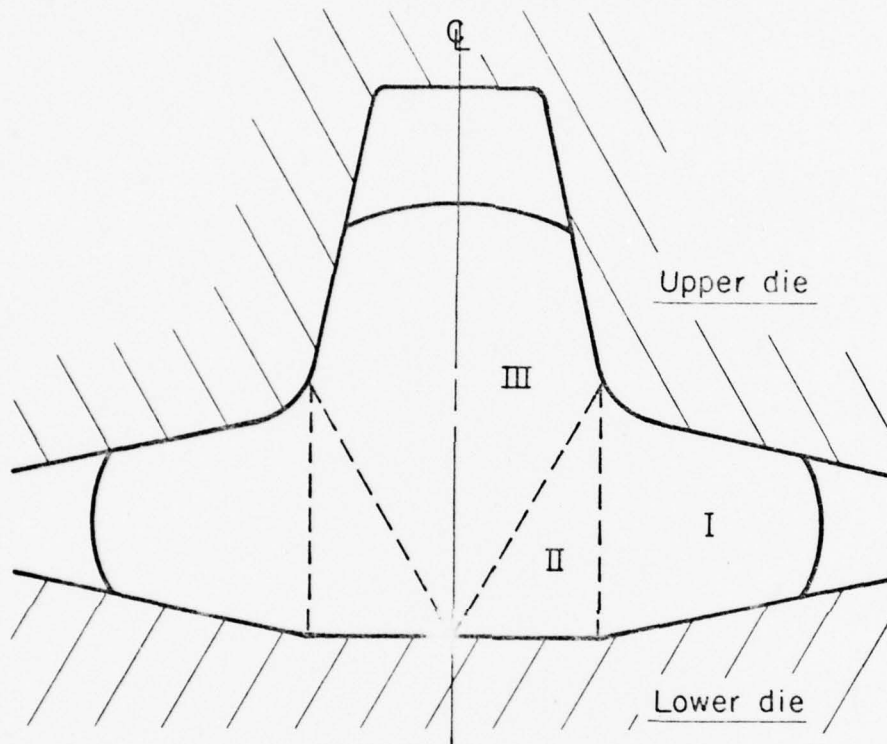
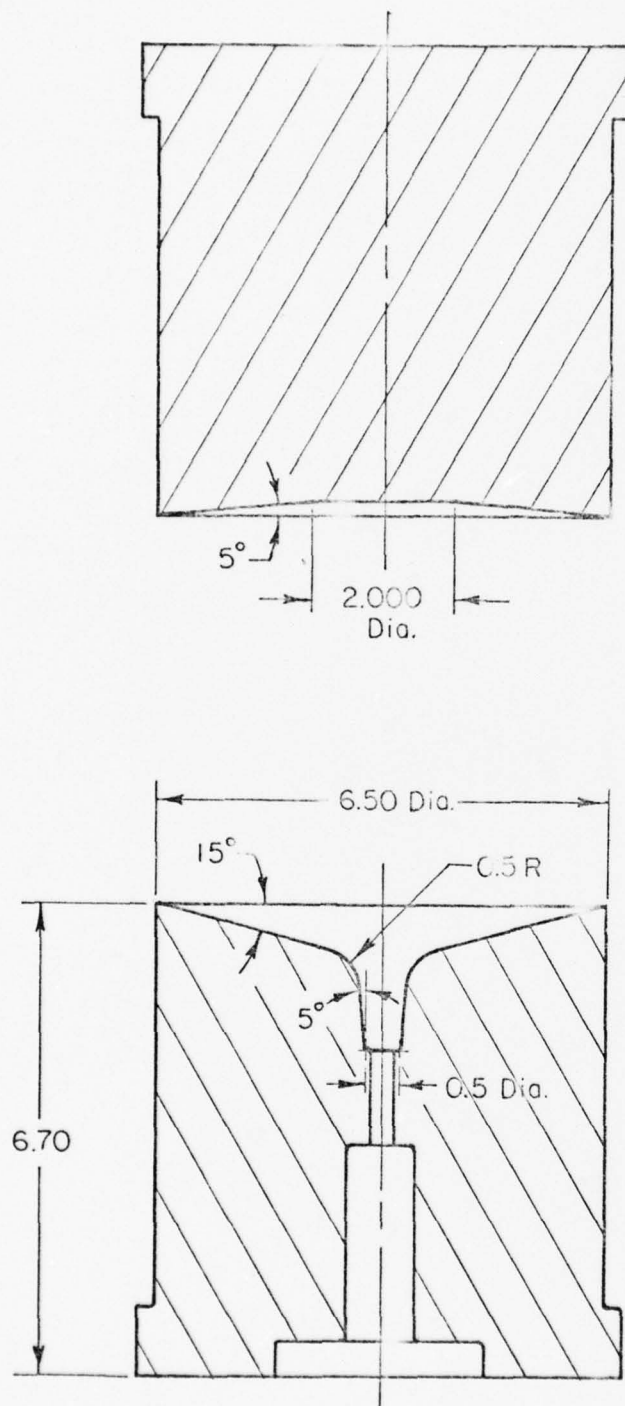FIGURE 6.1. REGIONS OF VELOCITY FIELD IN
EXTRUSION FORGING

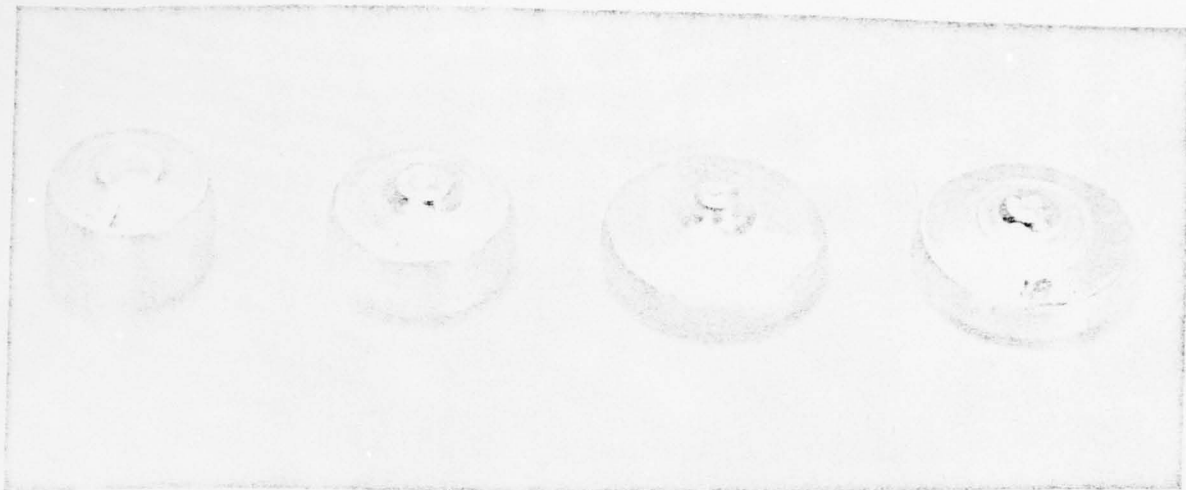FIGURE 6.2.   DIES FOR EXTRUSION FORGING TRIALS

38

FIGURE 6.3.   FORGED LEAD SPECIMENS

FIGURE 6.4.   FORGED ALUMINUM (1100) SPECIMENS

stroke were recorded with respect to time on the light beam oscillograph. The test results are summarized in Table 6.1.

After forging was completed, the specimens were cut along a diametral plane and their external profile was traced, as shown in Figures 6.5 and 6.6 for lead and aluminum specimens, respectively. As seen in Figure 6.5, the spike height and bulging of free surfaces increase with increasing reduction in height, but they decrease with decreasing friction (see specimen No. 18). Similar observations were also made in the case of aluminum specimens.

The oscillography recordings were degitized and plotted on z x-y recorder, as shown in Figure 6.7. The forging load increases slowly with increasing reduction in the initial stages. However, once a substantial spike is formed, the load increases rather rapidly. Further, the overall load-displacement curve moves up with increasing friction at the die-material interface.

The metal flow during these extrusion forging experiments were further studied by observing the cut specimens. The shape of the bulge profile, the formation of the dead-metal zone near the bottom die and development of the spike during forging were measured. This information was very useful in developing the mathematical-computer model, especially in terms of deciding the location of the neutral plane in the initial stages.

6.2. Analysis of Extrusion Forging

Due to inherent complexity in all forging processes, particularly in hot forging where the temperature and friction conditions can vary considerably across the workpiece, few analytical studies have been conducted in the past. These studies have been helpful in understanding and estimating the effect of interface friction upon metal flow in upset and extrusion-type forgings. However, in order to establish a realistic relation between the process variables and material response, the analysis of deformation must take into account the dependency of material behavior on strain, strain rate, and temperature. Also the analysis should supply complete information on these parameters so that the properties of the deformed material may be predicted.

TABLE 1. RESULTS FROM EXTRUSION FORGING TRIALS

| Specimen Number	Material	Lubricant	Die Temp. C	Specimen Temp. C	Reduction in Height percent	Forging Load metric ton	Final Height (including spike) mm
1	Al 1100-0	None	315	315	17.1	13.13	51.00
2	Al 1100-0	None	315	425	17.8	--	50.19
3	Al 1100-0	None	315	425	18.0	9.60	50.14
4	Al 1100-0	Fel-Pro C-300	315	425	17.3	11.53	50.67
5	Al 1100-0	Fel-Pro C-300	315	425	17.6	10.41	50.47
6	Al 1100-0	None	315	315	60.5	60.24	36.04
7	Al 1100-0	None	315	425	60.6	50.15	36.09
8	Al 1100-0	Fel-Pro C-300	315	425	60.9	41.10	30.35
9	Al 1100-0	None	315	315	45.9	29.60	38.15
10	Al 1100-0	None	315	425	46.3	20.28	37.64
11	Al 1100-0	Fel-Pro C-300	315	425	46.4	20.17	35.76
12	Al 1100-0	None	315	315	31.2	19.81	43.56
13	Al 1100-0	None	315	425	32.1	12.43	43.66
14	Al 1100-0	None	315	425	32.0	12.62	43.43
15	Lead	None	21	21	29.8	9.98	44.50
16	Lead	None	21	21	44.5	14.51	37.82
17	Lead	None	21	21	58.7	30.53	36.47
18	Lead	Fel-Pro C-300	21	21	58.8	26.31	32.13
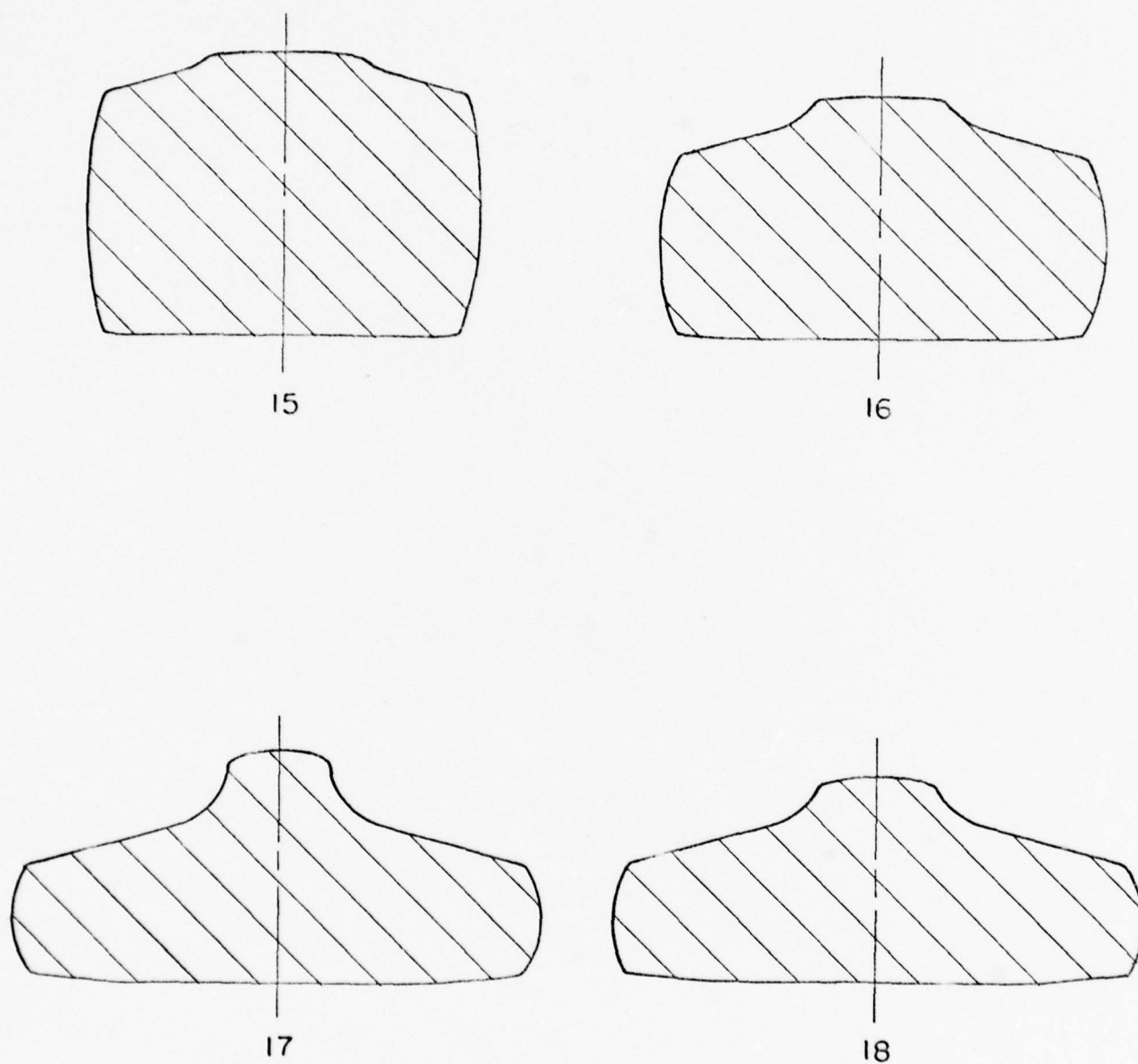
FIGURE 6.5. EXTERNAL PROFILE OF LEAD SPECIMENS AFTER FORGING AT ROOM TEMPERATURE

Specimens 15, 16 and 17 are forged without lubrication, specimen 18 was lubricated.
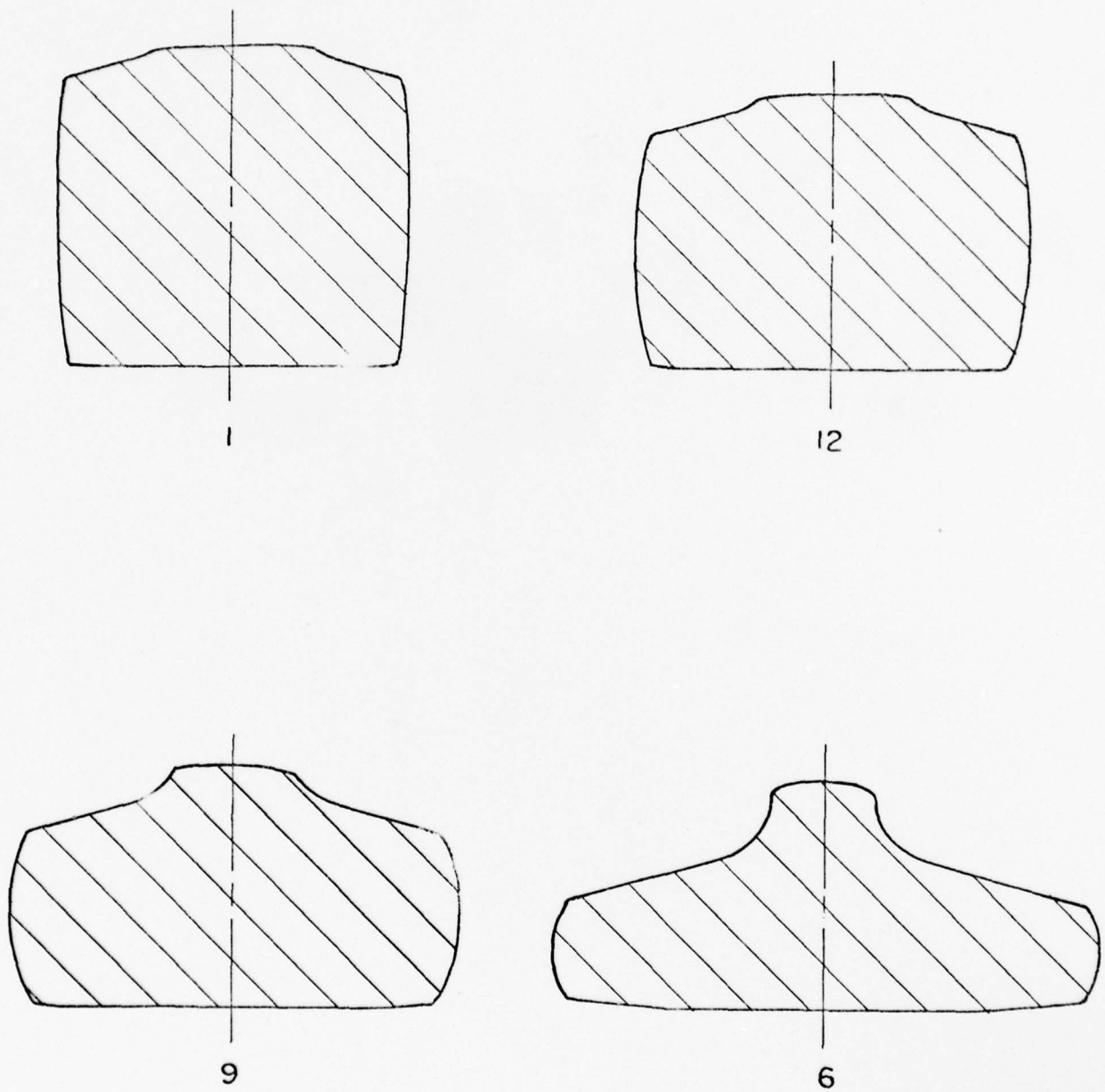
FIGURE 6.6 EXTERNAL PROFILES OF ALUMINUM SPECIMENS AFTER UNLUBRICATED
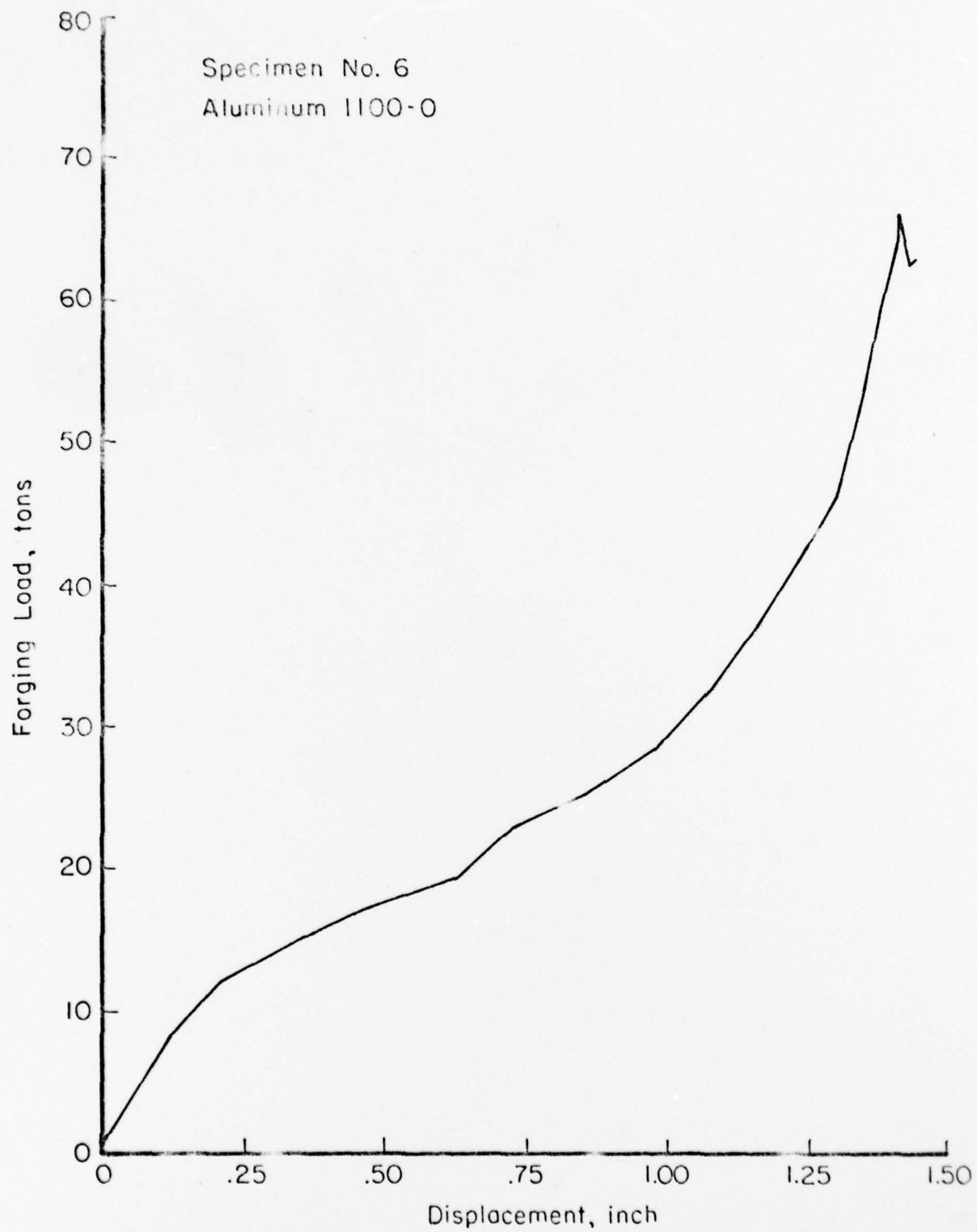ISOTHERMAL FORGING AT 600 F

FIGURE 6.7. A TYPICAL EXPERIMENTAL LOAD DISPLACEMENT CURVE IN EXTRUSION FORGING

In an effort to develop an algorithm to predict the velocity, strain, strain rate and temperature fields in axisymmetric forgings, an analysis of metal flow in an extrusion-type forging, shown in Figure 6.1, was undertaken. Here the metal flows both in the axial and the radial direction and the deformation is very inhomogeneous. The material in the extruded portion gets worked less than that in the rest of the forging. Consequently, the grain size is much coarser in the extruded portion compared to that in the portions of the forging directly under the compressive load, and this results in different properties at various locations of this type forging. In addition, the frictional constraint upon plastic deformation and metal flow also influences the microstructure. A study of the effects of various forging variables on material response in such a case has not been investigated. The geometry of the rigid dies, the speed of the machine, or the friction conditions can be selected such that the process can be optimized in terms of strain, strain rate, and temperature distributions in order to get the desired microstructural properties.

To analyze the metal flow in the extrusion-type forging, the upper-bound approach is used. In this case, however, defining the continuous velocity field in such a geometry is extremely difficult. Hence, the deformation zone is divided into a number of modular elements as shown in Figure 6.8. Velocity fields, which are kinematically admissible, were developed for each modular shape. The most important condition to be satisfied is that, when all the modules are assembled, the velocity conditions must satisfy all the boundary conditions and the condition of incompressibility. Upper-bound analysis by the modular elemental technique is not new, but almost all known earlier analyses using this technique were aimed at the estimation of forging loads. Further, in these analyses, even though the velocity field and strain rates were computed in order to estimate the deformation energy, the dependency of metal behavior upon strain, strain rate and temperature is ignored.

In the present study an improved upper-bound analysis, which includes the effect of strain, strain rate, and temperature, has been developed to predict the metal flow. As can be seen from Figure 6.8, the deformation zone basically consists of six different types of modules shown
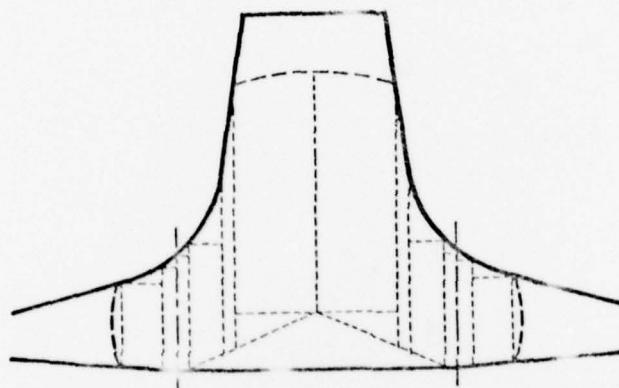
FIGURE 6.8. ELEMENTS FOR ANALYSIS OF METAL FLOW IN
EXTRUSION FORGING BY MODULAR UPPER-
BOUND APPROACH

in Figure 6.9. General expressions for continuous velocity components in each of these six elements have been formulated. For example, for a trapezoidal element shown in Figure 6.9c, the radial and axial velocity components can be expressed as:

$$U_r = \frac{1}{2rA} \left[U(r^2 - R_1^2) + \frac{2V}{tab} \right] \tag{1}$$

$$U_z = \frac{1}{rA^2} \left\{ U \left[Hr + (r^2 - R_1^2)^2 \frac{tab}{2} \right] - V \right\} \left(A + h - Z \right)$$

$$+ U_{z1} + U_r \tan \alpha \tag{2}$$

And, the effective strain rate is

$$\dot{\varepsilon} = \frac{2}{\sqrt{3}} \left\{ \frac{1}{8r^4 A^4} \left[L + 2 \left(- Z U(rA - \frac{CD}{A}) + V \frac{C}{A} \right) + M \right]^2 \right\}^{1/2} \tag{3}$$

where, in addition to the notations shown in Figure 6.9c, the variables L, M, A, B, C, D, U, V and tab are defined from the velocities and the geometry of the element.

In order to include the bulging of free surfaces due to friction at the tool-workpiece boundaries, special elements shown in Figure 6.9e and 6.9f have been developed. Similarly, the triangular element with curved boundary, shown in Figure 9d, eliminates the necessity for approximating the curved boundaries with small triangular elements.

6.3. Computer Programs for Metal Flow Analysis

A set of interactive computer programs called FORSIM has been developed for dividing the cross sections of a forging systematically into modular elements. Figure 6.9 is a computer display of the elements automatically divided by FORSIM.

Using the developed velocity field, FORSIM estimates strain rates within the modular elements using appropriate equations. Strains within the elements are obtained by integrating the continuous strain-rate functions with respect to time over the elapsed time interval. The

(a) Triangle

(b) Rectangle

(c) Trapezium

(d) Triangle with curved surface

(e) Rectangle with axial bulge
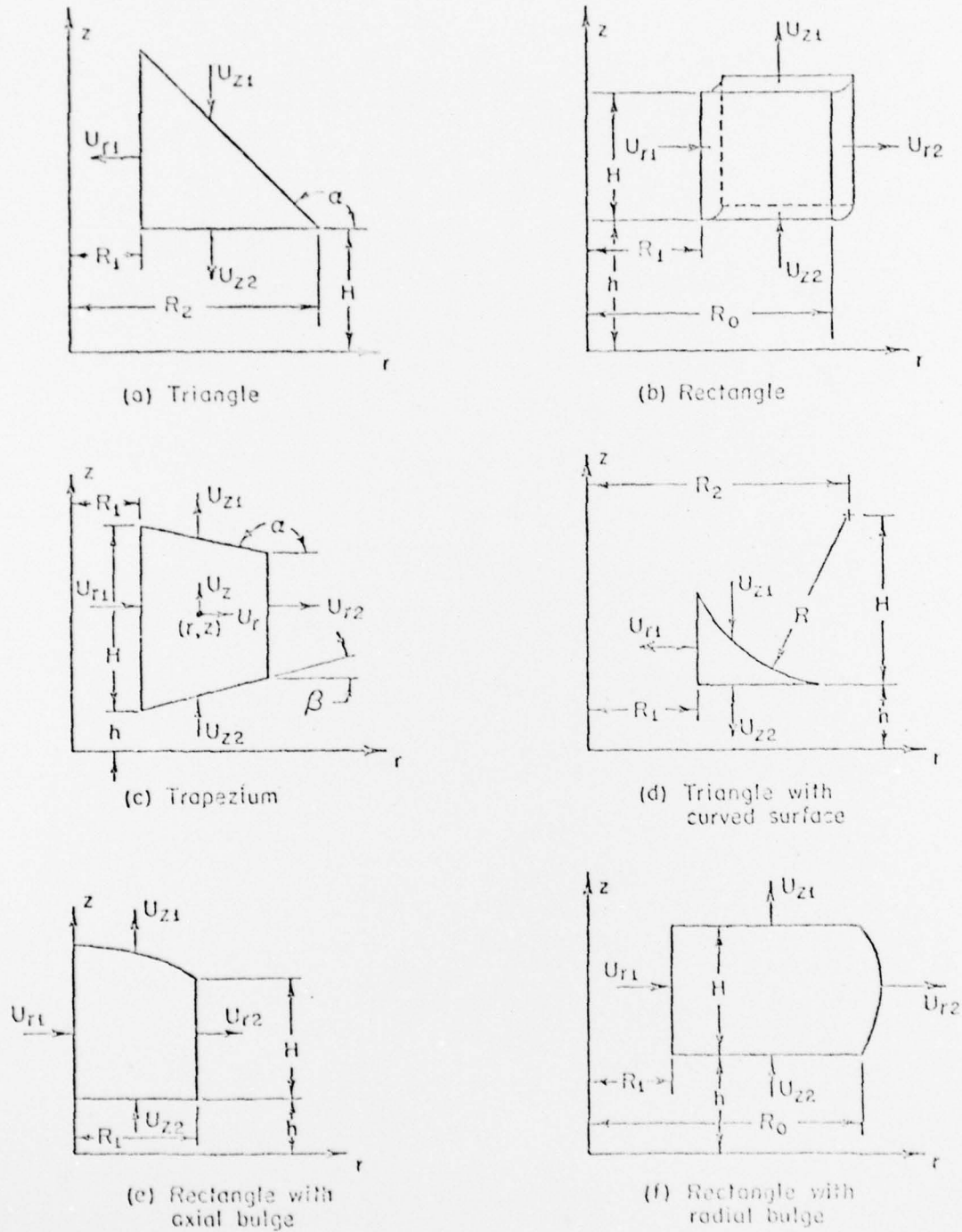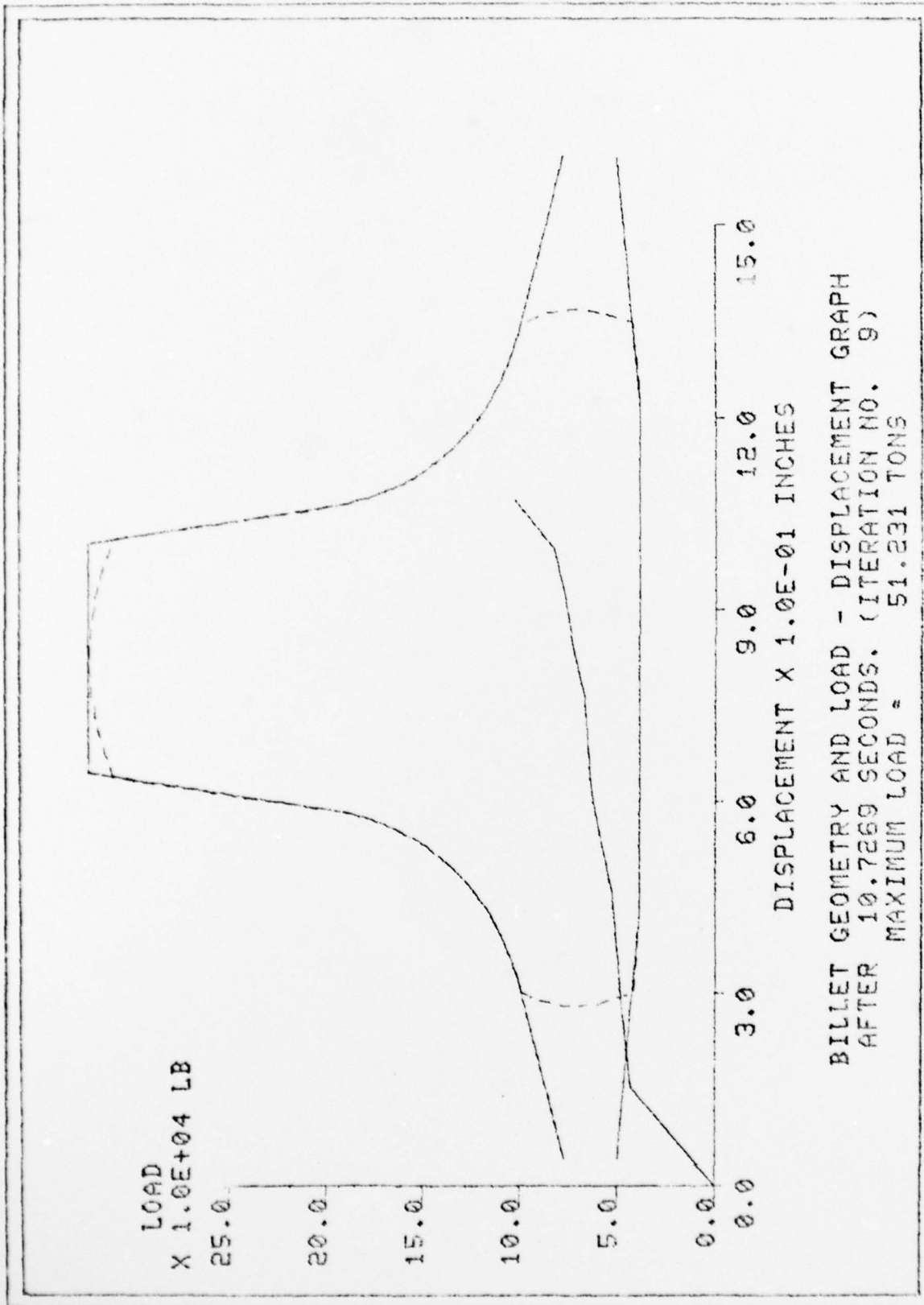
(f) Rectangle with radial bulge

FIGURE 6.9.   BASIC MODULAR ELEMENTS USED IN FORGING
SIMULATION

temperature analysis in this case is very involved. The problem under consideration is one of non-steady state heat transfer in a moving incompressible medium with heat sources. These calculations are best made by using numerical finite-difference or finite-element techniques. Due to very large requirements of computer time, temperature analysis is not incorporated at this time. However, Battelle plans to include the temperature analysis in FORSIM in the near future. Battelle is also conducting a program under Air Force Materials Laboratory sponsorship to develop process models for producing a dual property titanium alloy compressor disk. The basic objective of that program is similar to the present program. Therefore, Battelle will include the temperature analysis in FORSIM under the new Air Force Materials Laboratory program.

From the known velocity field, strain and strain rates, FORSIM calculates the total energy rate of plastic deformation. However, this estimation is based on assumed values for unknown parameters, such as the location of the neutral plane, the bulge profiles and the geometry of the dead metal zone. Hence, after the energy estimation, by an interactive procedure, the energy is minimized with respect to the unknown parameters. This procedure is repeated at several discrete steps of deformation in order to simulate the actual process.

At the end of each step, (or, as desired by the user) the deformation elements will be displayed as shown in Figure 6.8. Also, as seen in Figure 6.10, the instantaneous die position and the billet geometry are displayed along with the load-displacement curve. In addition, the elapsed time, maximum load and the iteration number are also displayed as additional information to the user.

Originally, FORSIM was developed on CDC 6500 computer for interactive use with Tektronix graphic display terminal as the input-output device. Because of the iterative nature, the minimization procedure requires considerable amount of computation time, making its iterative application uneconomical. Hence, FORSIM has now been modified into a hybrid system such that it can be used both interactively and in batch operation. If desired, FORSIM may be run in batch operation first, the results may then be stored in a permanent file and displayed later interactively.

FIGURE 6.10. BILLET GEOMETRY AND LOAD-DISPLACEMENT CURVE

In its present overlay structure, FORSIM requires less than 50K memory space. Though this system was developed for operation on CDC computer, most special functions which are unique to CDC system have been avoided. Thus, implementing FORSIM in systems other than the CDC system will require very minimum additional effort.

6.4. Strain Distribution in Extrusion Forging

Currently, the computer model is capable of predicting strains and strain rates in each element of the extrusion-type forging. The strain rate distribution is instantaneous, and it can be obtained at any moment during the forging operation. Strain rate distribution during forging is important since it determines and influences the microstructural changes occurring during deformation.

The strain in an element is cumulative in nature and influences the final microstructure as well as the final properties of the formed part. The strain distribution after 55 percent reduction in height in the extrusion forging experiment is shown in Figure 6.11. The modular upper-bound technique allows the determination of the strain distribution in each element, since the deformation path of each element during forging is known. As seen in Figure 6.11, the average overall logarithmic strain is 0.80, whereas the minimum and maximum strains vary between 0.36 and 1.10. Knowledge of such a strain distribution is essential in understanding the influence of deformation on the final microstructure and the properties of the forged product.

6.5. Microstructure of Ni Extrusion Forgings

Nickel specimens were extrusion forged at 900 and 1000 C using a similar die design to that shown in Figure 6.8 except that the extrusion die diameter was reduced to accommodate the smaller diameter nickel specimens. The nickel cylinders were 5.08 cm high by 2.54 cm diameter. The press set-up and speed was the same as for the aluminum specimens described earlier. The bottom die was heated to 225 C and the top die was heated to 170 C for all the tests.
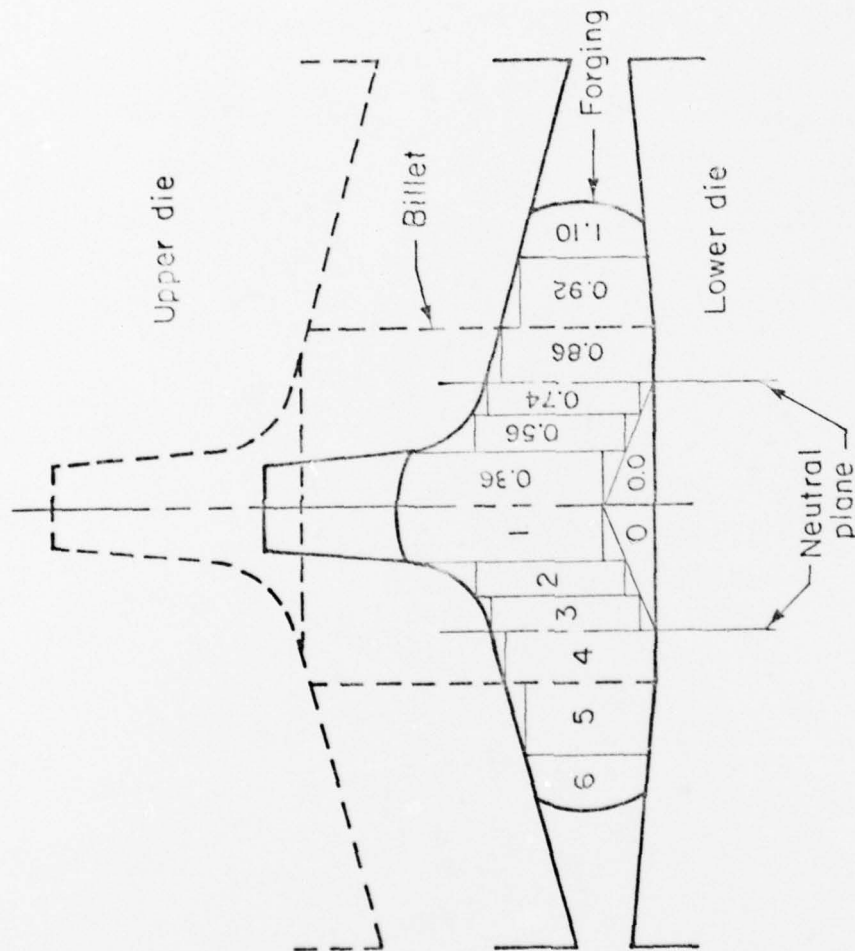
51

FIGURE 6.11. APPROXIMATE STRAIN DISTRIBUTION AFTER 55 PERCENT REDUCTION IN HEIGHT
(AVERAGE STRAIN = 0.8)

Numbers on the left hand side are element numbers and those on the
right hand side are strains in the elements.

The specimens were sectioned after forging to reductions of 26 and 64 percent and the microstructures were examined. The specimen profiles of a 900 C specimen extrusion forged to 64 percent reduction is shown in Figure 6.12a with the average grain sizes indicated on the different regions of the cross section. The grain sizes do not show much variation, except for a possible trend to lower grain size along the bottom of the specimen. This is presumably due to the cooler die lowering the temperature in this region. The most interesting result, after 64 percent reduction, showed the expected low strain zone under the extrusion opening in the top die. This zone was visible as a region of large grains caused by low-strain induced grain growth, shown bounded by the dashed line on the sectioned profile in Figure 6.12a. The microstructure of the region in the 900 C specimen is shown in Figure 6.12b. This low strain region illustrates the actual non-uniformity of the strain distribution in the low strain central column indicated in Figure 6.8. The tangient of fine grained material must originate from material in homogeneity, the 1000 C forgingins showed a similar but symetric large grained region. Clearly, even though the progress in analyzing complex forging shapes has been made, much more remains to be done before the non-uniformity of the resulting forged microstructures can be predicted.
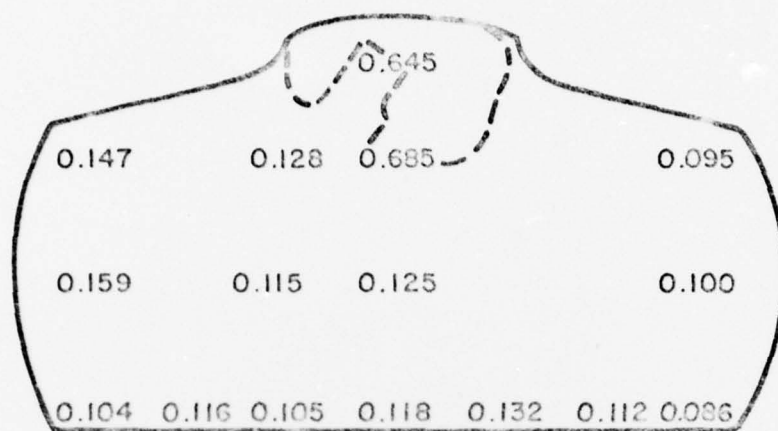
a. Profile of the extrusion forging. Large grained, low strain region is outlined by the dashed line. The grain size distribution is shown by the average linear intercepts (in mm) for different areas on the cross section. The profile is enlarged 2.5 times.

5X

b. Microstructure of the extrusion portion of the extrusion.

FIGURE 6.12. PROFILE AND MICROSTRUCTURE OF THE 900 C EXTRUSION FORGING OF NICKEL GIVEN A 64 PERCENT REDUCTION

7. CONCLUDING REMARKS

This program has made considerable progress towards developing a combined metallurgical/mechanics approach to the understanding of the forging process. It also identified some of the pitfalls in developing such an approach. The concept of microstructural marking was shown to be a promising tool for advanced metal working research. It can provide extremely useful insights into the detailed strain distribution in both simple and complex forgings. However, choice of a proper experimental material turned out to be a particularly difficult problem. Aluminum was found to be completely unsatisfactory but success was achieved with nickel. Nickel proved to be only a fair choice for studying high temperature workability criteria because of its high ducility in most situations of practical interest. Research on this grant did uncover the microstructural mechanism of high temperature failure and suggested the important role of environment in modifying strain- or strength-based fracture criterion.

Significant progress was made in the mathematical analysis of both ring and extrusion forgings but improvement in the comparison between the details of theoretical predictions and experiment needs to be made. These slight differences should not deter the further successful development of the process modeling techniques as they are being applied in the AFML forging program being carried out under the direction of Battelle-Columbus.

8. REFERENCES

Bishop, J.F.W., "An Approximate Method for Determining the Temperatures Reached in Steady-State Motion Problems in Plane Plastic Strains", Quarterly Journal of Mechanical and Applied Math, Vol. 9, (1956), p. 236.

Cramphorn, A. S., Bramley, A. N., and McDermott, R. G., "UBET Related Developments in Forging Analysis", NAMRC IV, Battelle's Columbus Laboratories, (1976).

DePierre, V. Curney, F., and Male, A. T., "Mathematical Calibration of the Ring Test with Bulge Formulation", Technical Report, AFML=TR=72-37,

Hahn, G. T., Barnes, C. R., and Rosenfield, A. R., "Influence of Microstructure and Second Phases on Fracture Toughness", Report ARL TR 75-0194 to Wright-Patterson AFB (1975).

Kuhn, H. A., and Dieter, G. E., "Workability in Bulk Forming Processes", Fracture 1977, Vol. 1, (1977), p. 307.

Ju, Kuang-shi, "A Modular Upper-Bound Method for the Analysis of Metal-Forming Problems", Ph.D. Thesis, Ohio State University,

Kobayashi, S., Lee, C. H., and Oh, S. I., "Workability Theory of Materials in Plastic Deformation Processes", AFML-TR-73-192, (May 1973).

Lahoti, G. D., Clauer, A. H., Rosenfield, A. R., and Altan, T., "Application of Process Modeling to Hot Isothermal Rolling of Titanium Alloy Strips", Proc. 1977 ASM Formability Symposium (in press).

Lahoti, G. D., and Altan, T., "Prediction of Temperature Distributions in Axisymmetric Compression and Torsion", Trans. ASME, Vol. 97, (1975), p. 113.

Lahoti, G. D., and Kobayashi, S., "On Hill's General Method of Analysis for Metalworking Processes", Institute International Journal of Mechanical Science, Vol. 16, (1974), p. 521.

Lee, C. H., and Altan, T., "Influence of Flow Stress and Friction Upon Metal Flow in Upset Forging of Rings and Cylinders", Journal of Engineering Industry, Trans. ASME, Series B, Vol. 94, (1972), p. 775.

Lee, P. W., and Kuhn, H. A., "Fracture in Cold Upset Forging -- A Criterion and Model", Metall. Trans., Vol. 4, (1973), p. 969.

Liu, J. Y., "An Analysis of Deformation Characteristics and Interfacial Frcition Condition in Simple Upsetting of Rings", ASME, Series B, Vol. 94, (1972), p. 1149.

Luton, M. J., and Sellars, . M., Acta Met., Vol. 17, (1969) p. 1033.

McDermott, R. P., and Bramley, A. N., "Forging Analysis -- A New Approach", NAMRC II, University of Wisconsin, (1974).

McQueen, H. J., and Hockett, J. E., Met. Trans., Vol. 1, (1970), p. 2907.

Nagpal, V., Lahoti, G. D., and Altan, T., ASME Paper 77-WA/PROD-35 (1977).

Pohl, W., "A Method for Approximate Calculation of Heat Generation and Transfer in Cold Upsetting of Metals", (in German), Dotoral dissertation, University of Stuttgart, (1972).

Rosenfield, A. R., "Diametrical Compression of Rings", Strain, Vol. 14, (1978), p. 150.

Shapiro, E., and Dieter, G. E., "Fracture and Ductility in Hot Torsion of Nickel", Metal. Trans., Vol. 2, (1971), p. 1385.

Wood, G. C., and Wright, I. G., "The Scaling of Nickel and Nickel-Cobalt Alloys in Air", Corrosion Science, Vol. 5, (1965), p. 841.